CEBAF PROPOSAL COVER SHEET

This Proposal must be mailed to:

CEBAF
Scientific Director's Office
12000 Jefferson Avenue
Newport News, VA 23606

and received on or before OCTOBER 31, 1989

A. TITLE: Measurement of $p(e,e'\pi^+)n$, $p(e,e'p)\pi^o$, and $n(e,e'\pi^-)p$ in the 2nd and 3rd Resonance Regions.

B. CONTACT PERSON: Ralph Minehart

ADDRESS, PHONE AND BITNET:

Institute of Nuclear and Particle Physics
University of Virginia, Charlottesville, VA
804/924-6785 MINEHART@VIRGINIA

C. THIS PROPOSAL IS BASED ON A PREVIOUSLY SUBMITTED LETTER OF INTENT

[X] YES
[ ] NO

IF YES, TITLE OF PREVIOUSLY SUBMITTED LETTER OF INTENT

Measurement of $p(e,e'^{+})$ and $n(e,e'^{-})p$ in the Second Resonance Region.

D. ATTACH A SEPARATE PAGE LISTING ALL COLLABORATION MEMBERS AND THEIR INSTITUTIONS

==========

(CEBAF USE ONLY)

Proposal Received 10-31-89

Log Number Assigned PR-89-038

By KES

contact: Minehart

Study of Electromagnetic Excitation of Baryon Resonances with the CEBAF Large Acceptance Spectrometer

The N* Collaboration

V. Burkert, D. Joyce, B. Mecking, M.D. Mestayer, B. Niczyporuk, E.S. Smith, A. Yegneswaran
CEBAF, Newport News, Virginia

R. Minehart, D. Day, J. McCarthy, O. Rondon-Aramayo, R. Sealock, S. Thornton, H.J. Weber
University of Virginia, Charlottesville, Virginia

P. Stoler, G. Adams, L. Ghedira, N. Mukhopadyay
Rensselaer Polytechnic Institute, Troy, New York

R. Arndt, D. Jenkins, D. Roper
Virginia Polytechnic Institute and State University, Blacksburg, Virginia

D. Isenhower, M. Sadler
Abilene Christian University, Abilene, Texas

D. Keane, M. Manley
Kent State University, Kent, Ohio

S. Dytman, T. Donoghue
University of Pittsburg, Pittsburg, Pennsylvania

C. Carlson, H. Funsten
College of William and Mary, Williamsburg, Virginia

D. Doughty
Christopher Newport College, Newport News, Virginia

L. Dennis, K. Kemper
Florida State University, Tallahassee, Florida

K. Giovanetti
James Madison University, Harrisonburg, Virginia

J. Lieb
George Mason University, Fairfax, Virginia

W. Kim
University of New Hampshire, Durham, New Hampshire

C. Stronach
Virginia State University, Petersburg, Virginia

M. Gai
Yale University, New Haven, Connecticut

Proposal 2

Measurements of $p(e,e'\pi^+)n$, $p(e,e'p)\pi^0$, and $n(e,e'\pi^-)p$ in the Second and Third Resonance Regions

The N*-Collaboration

R. Minehart, V. Burkert, M. Gai

Coordinators

ABSTRACT

We propose to scatter electrons from hydrogen and deuterium targets in the CLAS detector to study the single pion photoproduction reactions, $p(e,e'\pi^+)n$, $p(e,e'p)\pi^0$ and $d(e,e'\pi^-)pp_s$, in the region of the N* masses from 1350 to 1800 MeV. This is the first stage of a program which will ultimately include measurements with polarized beam and polarized targets. Our goal is the characterization of single pion electroproduction in the resonance region with a complete set of model independent amplitudes depending on $Q^2$and W. This first stage will already provide orders of magnitude improvement in the experimental data base, and is expected to play an important role in evaluating models used to describe the nucleon and its excited states.

Electrons with energies of 2 and 4 GeV will be scattered through angles from 10 to 45° to cover a range in Q^2 from 0.1 to 3 $(GeV/c)^2$. We are requesting 2000 hours (1000 hours for each target) at 4 GeV and 600 hours((300 hours for each target) at 2 GeV. We have assumed that CLAS will operate at a luminosity of 10^{34} $cm^{-2}sec^{-1}$ with proton and deuteron targets. The data can be obtained simultaneously with the data for other experiments using proton and deuteron targets at the CLAS.

I. Introduction and Physical Motivation

We propose to use the CLAS detector to study the single pion photoproduction reactions,

$$p(e, e'\pi^+)n, \qquad (1)$$

$$p(e, e'p)\pi^0, \qquad (2)$$

and

$$d(e, e'\pi^-)pp_s, \qquad (3)$$

on the proton and neutron (in the deuteron) in the region of the N* masses from 1350 to 1800 MeV.

Single pion electro-production is dominated by excitation of the nucleon to a resonant state which then decays to a nucleon and pion. The kinematics are determined completely by measuring the energy and angles of one of the hadrons in addition to the electron scattering parameters. The invariant mass, W, of the intermediate excited state of the nucleon depends only on the incident and final momentum of the electron, with

$$W^2 = M^2 + 2\nu \cdot M - Q^2, \qquad (4)$$

where M is the mass of the nucleon, ν is the energy lost by the scattered electron, and $-Q^2$ is the electron invariant momentum transfer. At fixed $Q^2 < 4$ (GeV/c)^2 the inclusive electron scattering cross section as a function of W, exhibits three distinct peaks for W between 1 and 2 GeV. The first and largest is due to excitation the $\Delta_{3,3}$ (or the $P_{33}(1232)$). The second peak around 1500 MeV is due primarily to the excitation of the $S_{11}(1535)$ and $D_{13}(1520)$ resonances. Excitation of a third N* in this mass region, the $P_{11}(1440)$, usually called the "Roper", has not been established for Q^2 less than 4 (GeV/c)^2, although it has been well established in photoproduction. The three N* states known to exist in the second resonance region all have isospin 1/2, and decay about half the time into a nucleon and a single pion. The third resonance region around 1700 MeV is known to be dominated by the $F_{15}(1690)$.

The cross section for production of single pions by unpolarized electrons on an unpolarized target is given by

$$\sigma_0 = \sigma_u + \epsilon\sigma_L + \epsilon\sigma_T \cos(2\phi) + (\frac{\epsilon(1+\epsilon)}{2})^{\frac{1}{2}}\sigma_I \cos\phi. \qquad (5)$$

where the various terms, σ_u, are functions of Q^2, W and θ_{cm}. The dependence on the out of plane angle, ϕ, is shown explicitly. The part independent of ϕ is split into two terms, the first depending on transverse photons and the second depending on longitudinal photons. It is known that the longitudinal part is generally small in the resonance region, of the

order of 10-20 %. It can only be determined by a Rosenbluth separation, i.e. by making measurements at two or more values of the polarization parameter, ϵ, while keeping W and Q^2 fixed. Since small systematic errors can lead to large errors in the subtracted longitudinal cross section, we prefer to postpone such measurements until the CLAS acceptance functions for different field settings are well understood. The ϕ dependent terms in the cross section are related to the real parts of interference terms between different helicity amplitudes, and will be of considerable importance in the analysis.

Most of the currently popular models of nucleon structure are QCD inspired quark models. These models are a first step in a program to derive a description of the nucleus from first priciples. We have, however, almost no knowledge even of the structure of the nucleon and its excited states. Until we have a firm understanding of the structure and dynamical behavior of this fundamental system, attempts to explain nuclear processes at a quark level seem premature. As stated by Close[1], the non-relativistic color quark model has been around for 20 years, has produced a highly successful phenomenology, notably through the work of Isgur and Karl[2], with very little theoretical justification, and it must be wrong. It is important to find out where the model breaks down. The photon is a clean probe that couples to the spin and flavor of the constituent quarks, and therefore can be expected to reveal correlations among flavors and spins.

I.B. Amplitudes Extracted from Data for Dominant N* States

The $S_{11}(1535)$, the $D_{13}(1520)$ and the $F_{15}(1690)$ states are of special interest since they stand out prominently even in inclusive electron scattering. Connection to theoretical models of the nucleon and its resonant states can be made most easily by extracting the transverse photo-coupling helicity amplitudes, $A_{\frac{1}{2}}$ and $A_{\frac{3}{2}}$, and the longitudinal photo-coupling helicity amplitude,$S_{\frac{1}{2}}$ (defined in the Appendix). The data have been reviewed and compared to calculations based on the non-relativistic quark model by Foster and Hughes[3]. Recently Pfeil[4] and his group, Mukhopadhyay[5], and Weber[6], among others, have been working to make the models more realistic. For the spin 1/2 states, S_{11} and P_{11}, only the $A_{\frac{1}{2}}$ and $S_{\frac{1}{2}}$ photo-coupling amplitudes are present. The results of calculations for $A_{\frac{1}{2}}$ and $S_{\frac{1}{2}}$ from Pfeil's group are shown in Fig. 1 for the $S_{11}(1535)$ and the $P_{11}(1470)$, along with extractions of the amplitudes from published data, which are subject to uncertainty due to the sparseness of the data. Pfeil's calculations deviate strongly from the non-relativistic calculations, and indicate a sensitivity to the shape of the quark confining potential. For these calculations, the transverse amplitude for the $S_{11}(1535)$, but not for the $P_{11}(1440)$, is sensitive to potential variations, whereas for the longitudinal amplitudes, the $P_{11}(1440)$ but not the $S_{11}(1535)$ is

sensitive.

The calculations of the amplitudes are sensitive to configuration mixing in the wave functions, as illustrated in Fig. 2, where calculations for $A_{\frac{1}{2}}$ for the $D_{13}(1520)$ and the $S_{11}(1650)$ are shown. Two different wave functions were used to determine the sensitivity to configuration mixing. It turns out that two resonances are sensitive to the configuration mixing at different values of Q^2, which, it is interesting to note, are accessible to the proposed experiment.

As discussed in the general introduction to the N* program, simple helicity arguments for the coupling of a photon and a quark suggest that at large Q^2, the helicity 1/2 amplitude must dominate. At low Q^2, it is known that both photoproduction and electroproduction of the $D_{13}(1520)$ and $F_{15}(1690)$ are pure 3/2. Thus one expects to see a transition from 3/2 to 1/2 as Q^2 increases towards QCD asymptopia. The quark models predict that this transition will occur in the region of Q^2 accessible at CEBAF. The helicity character of the production is most readily given by the ratio,

$$(A_{\frac{1}{2}} - A_{\frac{3}{2}})/(A_{\frac{1}{2}} + A_{\frac{3}{2}}),$$

which will change from -1 at $Q^2 = 0$ to the asymptotic value of +1 for large Q^2. Calculations, as well as analyses of existing data, not all of it published, are plotted in Fig. 3 and show this trend for the $D_{13}(1520)$ and the $F_{15}(1690)$. This figure also indicates sensitivity to the structure of the quark confining potential.

Because of the relative lack of competing channels, the study of the $S_{11}(1535)$ resonance through η production, as presented in another proposal from the Resonance group, is attractive. However, the lack of competing channels is related to the fact that the reaction is near the threshold for η production, where contributions from non-resonant direct η production may be important. The Kroll-Ruderman term (or seagull diagram) might give an S-like behavior that would rise at threshold and then drop off for larger invariant mass. Since the contribution is unknown, excitation of the S_{11} in pion production will help to determine the importance of this effect in η production.

The third resonance region contains many states with N=2 in the non-relativistic quark model. Measurement of the electroproduction of these states will provide an important test of single quark transition models. The only N=2 state in a lower mass region is the Roper, which as we will show in the following section, has many interesting, but peculiar properties.

I.d. The Roper Resonance

The Roper resonance has for a long time presented a variety of puzzles to nucleon spectroscopy. A forward peak in πp and pp excitation reactions has led to speculations that the

bump in the Roper region is only partly due to a P_{11} resonance. A phase shift analysis of Arndt et al.[7] tended to support the existence of two resonances in this region. Analyses of Hohler et al.[8], do not require two resonances, and there seems to be some agreement now that the Roper is probably a single resonance. The first calculations with the nonrelativistic quark model[2], which had great success in describing the $\Delta(1232)$ as a quark spin-flip excitation of the nucleon, motivated the description of the Roper as a quark radial excitation. These calculations yielded a photoproduction amplitude that was too small and the wrong sign. The calculated decay widths were also too narrow. More complicated models have been more successful.

It is interesting to note that while the Roper has been observed in photoproduction, its electroproduction not been established for Q^2 <3 $(GeV/c)^2$. It is possible that, although weakly excited, it may stand out more prominently in the separated longitudinal cross section terms, since as a radially excited state, the $P_{11}(1440)$ is predicted to have a strong longitudinal excitation. Recent calculations by Pfeil's group[4] support the idea that the longitudinal coupling is important for the Roper. Compilations[9] of the separated longitudinal and transverse electroproduction cross sections in the range of Q^2=1 $(GeV/c)^2$ generally find the ratio σ_L and σ_T <20 % throughout the resonance region. However, in the Roper region these compliations suggest an unusually large longitudinal component for the cross section, as shown in Fig. 4. Verification of a large longitudinal coupling for electroproduction of the Roper would be of great importance to the nucleon models. Although polarization terms are not accessible for our first measurements, it should be mentioned that the analysis of Kroesen[10] indicates that the longitudinal coupling to the Roper resonance may produce strong effects in cross section terms that can be accessed by polarization measurements.

As mentioned in the general introduction, it has been pointed out by Pfeil[4] that the ratio of $A_{\frac{1}{2}}$ amplitudes for the neutron and the proton excitation should be -2/3 if the transition were a magnetic excitation of the [56,0^+] group in the quark model. Testing this prediction requires the use of a neutron target.

I.e. Parity Doubling

Iachello[11] has proposed for the resonance structure the notion of parity doubling, which he suggests to be a consequence of the geometrical shape and the collective motion of the three quark system, resulting in reflection asymmetry. Whether these ideas can lead to distinct signatures in the electromagnetic form factors of the resonant states is not established but measurements of the production of states in the second and third region ultimately may play a role in testing these ideas.

II. Previous Measurements

Exclusive measurements of single meson production[12] in the resonance region have been carried out, mainly with proton targets (mostly at NINA, DESY and Bonn), using pairs of spectrometers to measure the electron and a hadron. No measurements using either polarized beams or polarized targets have been performed. In addition to the pion production reactions, eq. 1 and 2, the reaction p(e,e'p)η has been studied. Identification of these reactions requires the calculation of the mass of the missing neutral hadron. Previous measurements were carried out with two magnetic spectrometers and obtained typical missing mass resolutions of 150 MeV, FWHM, with signal to background ratios of 4 to 1 in the pion peak. Because of the limited solid angle coverage of the spectrometers, complete measurements of the distributions over the resonance decay angles exist in only a few selected cases.

Because of the limited amount of data on pion electroproduction, extraction of the photo-coupling helicity amplitudes is very sensitive to model dependence and limited to the prominent resonances. Aside from the three prominent resonances, there are at least seven other well established π-N resonant states with masses below 1800 MeV, for which the electromagnetic couplings, while important tests of nucleon spectroscopy, are not well known.

The measurements were made at relatively low luminosities, typically 10^{35} cm^{-2} sec^{-1}, with low acceptance spectrometers. We expect that the CLAS detector can operate with proton targets at luminosities of 10^{34} cm^{-2} sec^{-1}. When this is combined with its large acceptance, orders of magnitude improvement in the quality of the data can be expected. This is illustrated in Fig. 5, where cross sections measured at DESY and NINA for Q^2=1 (GeV/c)^2 are shown for W =1.5 GeV as functions of $\cos\theta_{cm}$ and ϕ_{cm}. Also shown are the results of a fit to the existing data by Kroesen[11], along with data points projected for our experiment. The stastical errors for the projected data are what we expect near the upper Q^2 limit for our measurements. The impressive improvement expected from the CLAS detector not only justifies our programmatic approach to the study of electroproduction of nucleon resonances, but guarantees impressive improvements in our knowledge of the pion electroproduction after a relative short experiment.

No coincidence measurements have been made with polarized beams or targets. A phenomelogical analysis of NINA and DESY data for $\gamma_v p \rightarrow \pi^+ n$ at Q^2=1 (GeV/c)^2 by Kroesen[11] shows that strong dependence of the cross section on various orientations of the target polarization may be expected. In particular, some polarization terms appear to be extremely sensitive to the longitudinal part of the Roper resonance.

TABLE I

Targets (Unpolarized)	H_2 D_2
E_0	2 GeV, 4 GeV
Θ_e	12^0 to $>45^0$
Q^2	0.1 $(GeV/c)^2$ - 3.0 $(GeV/c)^2$
W	1.35 GeV - 1.8 GeV
Δ Q^2	0.2 $(GeV/c)^2$
Δ W	20 MeV
Θ^*	Full range
ϕ	Full range

To estimate the response of the CLAS to the reactions of interest, we have used the CELEG event generator to generate a random set of inelastic electron scattering events for W<2 GeV. These events were analyzed with the FASTMC program to simulate the response of the CLAS detector. The CELEG event generator is a semi-classical calculation that includes only transverse terms, and does not generate interference terms. Moreover, at the present time it does not include background from Born terms and higher resonances. CELEG and FASTMC are consequently primarily useful for studying the expected experimental resolutions, and structure of the CLAS acceptance for particular reactions.

Extensive results of the CELEG-FASTMC calculations for some typical cases using a proton target are shown in Figs. 6 and 7. The first set of figures were obtained with E_0=4 GeV, with elastic ep scattering and all events for Q^2 <1 $(GeV/c)^2$ deleted from the generator. Results for the reactions, $p(e,e'\pi^+)n$ and $p(e,e'\ p)\pi^0$ are shown. The distributed kinematical quantities were calculated in two ways, first by using the exact particle momenta and angles provided by CELEG, and secondly, by using the "smeared" values to account approximately for the resolution of the CLAS magnet and wire chamber system. The polarity of the CLAS was chosen to bend negative particles towards the beam, and full field intensity was used.

From these calculations some general conclusions can be drawn. It is clear that the resolution in Q^2, W, and missing mass is much better than obtained in earlier experiments with conventional spectrometers. The CLAS acceptance for detection of single pion production is typically about 40%. The acceptance function depends both on $\cos\theta^*$ and ϕ, and consequently must be determined with precision. Results for the acceptance as a function of each of these angle variables are shown in Fig. 8. Comparison of figures for generated angles and smeared accepted angles shows that the distortion in $\cos\theta^*$ is generally less pronounced than

TABLE I

Targets (Unpolarized)	H_2 D_2
E_0	2 GeV, 4 GeV
Θ_e	12^0 to $>45^0$
Q^2	0.1 $(GeV/c)^2$ - 3.0 $(GeV/c)^2$
W	1.35 GeV - 1.8 GeV
Δ Q^2	0.2 $(GeV/c)^2$
Δ W	20 MeV
Θ^*	Full range
ϕ	Full range

To estimate the response of the CLAS to the reactions of interest, we have used the CELEG event generator to generate a random set of inelastic electron scattering events for W<2 GeV. These events were analyzed with the FASTMC program to simulate the response of the CLAS detector. The CELEG event generator is a semi-classical calculation that includes only transverse terms, and does not generate interference terms. Moreover, at the present time it does not include background from Born terms and higher resonances. CELEG and FASTMC are consequently primarily useful for studying the expected experimental resolutions, and structure of the CLAS acceptance for particular reactions.

Extensive results of the CELEG-FASTMC calculations for some typical cases using a proton target are shown in Figs. 6 and 7. The first set of figures were obtained with E_0=4 GeV, with elastic ep scattering and all events for Q^2 <1 $(GeV/c)^2$ deleted from the generator. Results for the reactions, $p(e,e'\pi^+)n$ and $p(e,e'\ p)\pi^0$ are shown. The distributed kinematical quantities were calculated in two ways, first by using the exact particle momenta and angles provided by CELEG, and secondly, by using the "smeared" values to account approximately for the resolution of the CLAS magnet and wire chamber system. The polarity of the CLAS was chosen to bend negative particles towards the beam, and full field intensity was used.

From these calculations some general conclusions can be drawn. It is clear that the resolution in Q^2, W, and missing mass is much better than obtained in earlier experiments with conventional spectrometers. The CLAS acceptance for detection of single pion production is typically about 40%. The acceptance function depends both on $\cos\theta^*$ and ϕ, and consequently must be determined with precision. Results for the acceptance as a function of each of these angle variables are shown in Fig. 8. Comparison of figures for generated angles and smeared accepted angles shows that the distortion in $\cos\theta^*$ is generally less pronounced than

the distortion in ϕ. This latter distortion is due to the fact that ϕ represents the rotation of the decay momentum around the $\vec{q}$ vector, and for $\phi = 180^0$, the decay pion is moving forward in the CLAS where there is a high probability that it will be lost in the open region around the beam line. The calculations also indicate that the resolution of CLAS is excellent.

The CELEG program also can generate events with Fermi momentum of the struck nucleon folded in. We have used this feature to generate a set of data to simulate resonance production in the deuteron. Typical results are shown in Fig. 9. It is clear that the Fermi momentum introduces serious difficulties in the analysis of the data. Because of the potentially great value in studying the excitation of the neutron, it is important to pursue this measurement. We expect that an equal amount of time is needed for both proton and deuteron targets.

The program, ASYCALC, written by Kroesen[11], uses resonance amplitudes and Born terms that have been fit to world data (DESY, NINA and Bonn) at $Q^2 = 1$ (GeV/c)^2 to calculate cross sections for single pion electroproduction. We have used this program to study the sensitivity of the unpolarized cross sections to some selected helicity amplitudes. Since the Kroesen analysis is based on a limited and imperfect data set, these studies must be treated with caution. Nevertheless, they should be of some value in determining the required statistical accuracy. In Figs.10-12, the effects of deleting selected resonance amplitudes from the cross section are displayed. The error bars shown are an estimate of what we expect to obtain for our worst case, $Q^2 \approx 3$ (GeV)^2. Two observations can be made. First, the effects of individual terms are small, so that the proposed accuracy is definitely needed. Secondly, measurement of ϕ dependence provides information distinctly different from what can be learned from the θ dependence at a fixed value of ϕ.

IV. Future Measurements with Polarized Targets

Following completion of experiments with unpolarized targets, we want to use a polarized electron beam with polarized targets. With polarization measurements it is possible to extract additional spin-dependent amplitudes. In particular, imaginary parts of the amplitudes can be measured. We expect that low temperature polarized NH_3 and ND_3 targets will be used. With present technology these targets can be used at luminosities up to 3×10^{34} $cm^{-2}sec^{-1}$. It is clear that the maximum luminosity of the CLAS and the polarized targets are well matched. The large acceptance of the CLAS maximises the information obtained from the electron-target interactions. The polarization information from a complete 4π measurement is greatly enhanced over what can be obtained from the more traditional two spectrometers in coincidence, with their corresponding limitations, particularly for out of

plane measurements. There is room in the CLAS for insertion of a polarized target. The large magnetic field associated with the target will cause some changes in the particle trajectories, but these effects can be accounted for. It appears that all the measurements can be made with the target polarized along the beam so that the primary electrons will not be deflected.

V. Estimated Running Time

V.a. Unpolarized Measurements for 1.0 $(GeV/c)^2 < Q^2 < 3.0\ (GeV/c)^2$

The running time needed for this program is determined by the largest Q^2 desired. At the present time, measurements up to 3 $(GeV/c)^2$ appear feasible. We have estimated the beam time by using a compilation of Bodek[13] for the inclusive electron scattering cross section, combined with CELEG and FASTMC to get the acceptance fraction. The following assumptions were used:

- incident electron energy = 4 GeV
- luminosity = $10^{34}\ cm^{-2}$
- scattered electrons detected in the proposed CLAS shower detector, which extends to 45^0.
- binning of scattered electrons: Δ W = 0.02 GeV, $\Delta Q^2 = 0.25\ (GeV/c)^2$.

Under these assumptions, the number of counts obtained in 1000 hours for the two pion production reactions on the proton in the Q^2 bin from 2.75 to 3 $(GeV/c)^2$:

W	$p(e,e'\pi^+)n$	$p(e,e'\ p)\pi^0$
1.4-1.6	60,000	40,000
1.6-1.8	20,000	20,000

If these events were sorted into 20 $\cos\theta^*$ and 20 ϕ bins, there would be 50 to 150 events per bin. This number of counts represents the threshold for extracting useful information about the resonance production amplitudes. At lower values of Q^2 the number of events is, of course, much greater.

V.b. Low Q^2 Measurements

In addition to the beam time requested at 4 GeV, we intend to run for a short time at 2 GeV for each experiment in order to study the transition form factors for Q^2 ranging from 0.1 to 1.0 $(GeV/c)^2$. This will allow a closer connection to the photoproduction data, which could be very important, especially for the case of the Roper, which is observed in photoproduction but has not been seen in electroproduction at low Q^2. For these measurements, the magnetic field in the CLAS will be reduced. CELEG and FASTMC simulations of this operating condition show no significant degradation of the resolution from that obtained at higher energies with full field. The beam time required for these measurements will be small, of the order of 300 hours.

V. c. Estimates for future polarized target experiments.

To determine in a preliminary way the practicality of the long-term program of polarization measurements, estimates of the quantity of data needed to analyze small components in the angular distributions were made with a Monte Carlo program based on the analysis of Kroesen[15] of existing data at 1 $(GeV/c)^2$. It was assumed that the data would be analyzed in terms of spherical harmonic terms. The calculations indicate that important polarization effects will show up in the spherical harmonic coefficients at the level of a few percent of the leading coefficient. To determine these coefficients to within a few percent of themselves, it appears that at least 10^5 events are needed in each Q^2 and W bin, essentially the same as we hope to get at the highest Q^2 with unpolarized targets. Since the polarization effects are expected to vary strongly from one resonance to another, relatively small bin sizes, of the order of 0.02 to 0.04 GeV in W are needed. Since the Q^2 dependence of different resonances

in this region can be expected to be quite different, bins of 0.2 $(GeV/c)^2$ in Q^2 are also desirable. As with the unpolarized measurements, the beam time needed for this program is determined by the largest Q^2 desired. Depending on the polarization of the beam and target, it appears that a minimum of 1500 hours will be needed for a proton target run with the target polarized parallel and anti-parallel to the beam. Measurements with other orientations will probably be unnecessary.

VI. Resolution Requirements

The CLAS will allow us to measure Q^2 to an accuracy of about 1% (fwhm). The invariant mass, W, can be calculated with an uncertainty of about 10 MeV (fwhm), The resonance decay angles will be measured with high precision, typically 0.003 (fwhm) for $\cos\theta^*$ and 0.5^0 (fwhm) for ϕ. It is important to calculate the final state missing mass accurately enough to eliminate two-pion final states from the data. The FASTMC analysis indicates that a missing proton mass can be calculated with a precision of about 2% (fwhm) and that a missing pion mass can be calculated to about 10% (fwhm). It is apparent that the CLAS will be an excellent instrument for these measurements.

VII. Trigger Requirements

The signal for the CLAS trigger will consist of an electron whose energy and angle is consistent with the Q^2 range and resonance mass, W. It is likely that most of the electrons identified by the forward shower counter will be used, because of requirements of other simultaneous experiments. As discussed in the general introduction, the single electron event rate is not likely to overburden the data acquistion system. However, if there is a problem with rates, our trigger can also include a requirement for a charged hadron in coincidence with the electron. If this is used, a fraction of events without the requirement of a detected hadron will also be taken, in order to calibrate the response of CLAS to inclusive electron scattering, and to determine the elastic scattering cross section.

VIII. Data Analysis

It is expected that much of the analysis will be carried out using computers at the University of Virginia, where there now is a Micro-Vax II with a dedicated 8 mm tape transport, and a DEC Station 2000, as well as a fraction of a VAX 11/780, and a VAX Station 3500 available for the N^* program. The system includes several 6400 cpi magnetic tape drives and a large amount of disk space, with more than 300 Mbytes presently available

for data analysis. The University of Virginia plans to acquire additional fast processors and disk facilities for data reduction between now and the time these experiments are run.

IX. Summary

We propose to use the CLAS to study the electroproduction of the nucleon resonances in the neighborhood of 1400 - 1800 MeV for $Q^2 < 3$ $(GeV/c)^2$ in a series of experiments:

1) Unpolarized beam on unpolarized proton target:
   1000 hours ($E_0 = 4$ GeV), 300 hours ($E_0 = 2$ GeV)
2) Unpolarized beam on unpolarized deuteron target:
   1000 hours ($E_0 = 4$ GeV), 300 hours ($E_0 = 2$ GeV)

It should be noted that while the extensive demand on the CEBAF facilities and beam time is well justified by the physics of nucleon resonance excitation, other CLAS experiments using the same targets can run simultaneously.

References

1. F.E. Close, Proceedings of the 1989 Summer Workshop, CEBAF.
2. N. Isgur and G. Karl; Phys. Rev. D18(1978)4187; ibid D19(1979)2653.
3. F. Foster and G. Hughes, Rep. Prog. Phys. **46**,1445 (1983).
4. M. Warns, W. Pfeil, and H. Rollnik, to be published in Z. Phys. C.
   M. Warns, H. Schroeder, W. Pfeil, H. Rollnik, BONN-ME-89-03-04(1989), to be published.
5. N. Mukhophadyay and Benmerrouche, Proc. Excited Baryons Conf., RPI, (1989), pub. World Press.
6. H.-J. Weber, Ann. Phys. **177**,38 (1987).
   Z. Phys. **A297**,261, (1980),
   W. Konen and H.-J. Weber, U. Va. Preprint, INPP-89-6, to be published.
7. R.A. Arndt, J.M. Ford, and L.D. Roper, Phys. Rev. **D32**, 1085 (1985).
8. G. Hohler, Few Body Conference, 1989, Vancouver.
9. F.W. Brasse et al., Nucl. Phys. **B110**, 410 (1976).
10. G. Kroesen, BONN-IR-83-3 (1983) (unpublished).
11. F. Iachello, Phys. Rev. Lett. **21**, 2440, (1989).
12 J.-C. Alder et al., Nucl. Phys., **B99**, 1 (1975).
   J.-C. Alder et al., Nucl. Phys., **B105**, 253 (1976).
   J.-C. Alder et al., Nucl. Phys., **B91**, 386 (1976).
   T.A. Armstrong et al., Phys. Rev. **D5**, 1640 (1972).
   B. Gerhardt et al., Z. Phys.,**C7**,11 (1980).
   J. Drees et al., Z.Phys.,**C7**, 183 (1981).
   W. Albrecht et al., Nucl. Phys., **B25**, 1 (1971).
   W. Albrecht et al., Nucl. Phys., bfB27, 615 (1971).
   W. Ash et al., Phys. Lett. **24B**, 165 (1967).
   P. Noelle et al., Nucl. Phys. **B26**, 461 (1971)
   H. Breuker et al., Z. Phys. **C13**, 113 (1982).
   H. Breuker et al., Z. Phys. **C17**, 121 (1983).
13. A. Bodek et al.,Phys. Rev. **D20**, 1471 (1979).

Figure Captions

1. Q^2 dependence of $A_{\frac{1}{2}}$ for the $S_{11}(1535)$ and the $P_{11}(1470)$, along with predictions of a relativistic quark model[4] for different choices of confining potential. The dashed lines show the results of the non-relativistic quark model.
2. Q^2 dependence of the ratio, $A_{\frac{1}{2}}/A_{\frac{3}{2}}$, for the D_{13} and $F_{15}(1690)$ resonances.
3. Helicity asymmetry, $(A_{1/2} - A_{3/2})/(A_{1/2} + A_{3/2})$, for the $D_{13}(1520)$ and $F_{15}(1690)$ resonances. Solid curves are calculations of Warn et al. for a constant confining potential, the dash-dot curve has a confining potential with an $r^{0.1}$ dependance. The other curve is the result of a non-relativistic calculation.
4. Ratio of longitudinal to transverse cross sections in the resonance region for Q^2 near 1 $(GeV/c)^2$, from Brasse et al.
5. Plot of cross sections for electroproduction of π^+ obtained from compilations of data from NINA and DESY at W = 1500 ± 30 MeV and $Q^2 = 1$ $(GeV/c)^2$ vs. $\cos\theta^*$ for 8 ϕ bins. For comparison, we show the calculations from fits to data obtained with the program, ASYCALC, written by Kroesen. Also shown are the projected results from our proposed experiment.
6. Simulated results from CLAS using the computer programs, CELEG and FASTMC, for the reaction, $p(e,e'\pi^+)n$ at the incident electron energy, $E_0 = 4$ GeV. Elastic ep scattering and all events for $Q^2 < 1$ $(GeV/c)^2$ were deleted from the simulation.
7. Same as Fig. 5, except for the reaction, $p(e,e'\ p)\pi^0$.
8. Efficiency for detection of single meson production reactions in the second resonance region, as a function of $\cos\theta^*$ and as a function of ϕ^*.
9. Simulated results from CLAS using the computer programs, CELEG and FASTMC, for the reaction, $d(e,e'\pi^-)pn$ at the incident electron energy, $E_0 = 4$ GeV. Quasi-elastic ep scattering and all events for $Q^2 < 1$ $(GeV/c)^2$ were deleted from the simulation.
10. Calculation of cross section at $Q^2 = 1$ $(GeV/c)^2$ using the program ASYCALC at three values of ϕ and twenty values of θ. The plots show the best fit cross section as compared to the cross section with $A_{\frac{1}{2}}$ for the Roper resonance set to 0. The error bars shown are an estimate of the experimental error expected for the proposed experiment at the highest values of Q^2.(Worst case)
11. Calculation of cross section at $Q^2 = 1$ $(GeV/c)^2$ using the program ASYCALC at three values of ϕ and twenty values of θ. The plots show the best fit cross section as compared to the cross section with $A_{\frac{1}{2}}$ for the $S_{11)}(1535)$ resonance set to 0. The error bars shown are an estimate of the experimental error expected for the proposed experiment at the highest values of Q^2.(Worst case)

12. Calculation of cross section at $Q^2 = 1$ $(GeV/c)^2$ using the program ASYCALC at three values of ϕ and twenty values of θ. The plots show the best fit cross section as compared to the cross section with $A_{\frac{1}{2}}$ for the $F_{15}(1690)$ resonance set to 0. The error bars shown are an estimate of the experimental error expected for the proposed experiment at the highest values of Q^2.(Worst case)

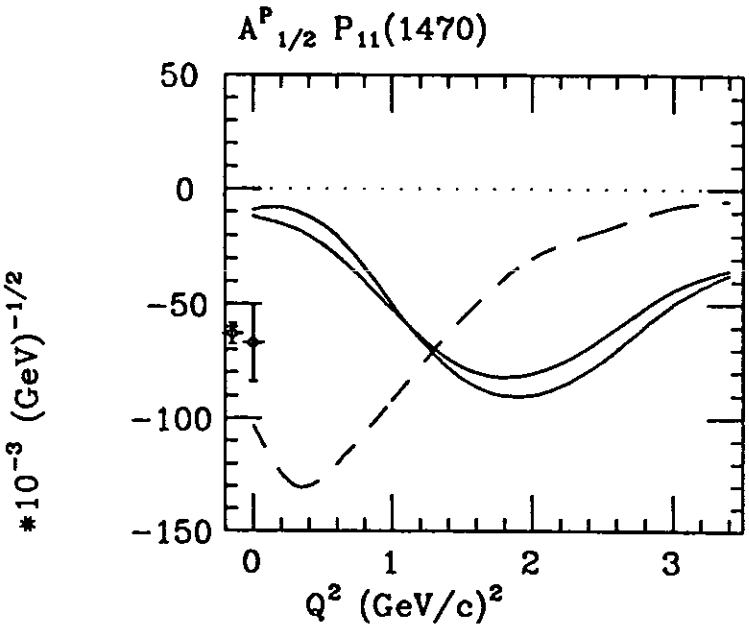
$A^P_{1/2}$ $P_{11}(1470)$
50
0
−50
−100
−150
0
1
2
3
Q^2 (GeV/c)^2
$*10^{-3}$ (GeV)$^{-1/2}$

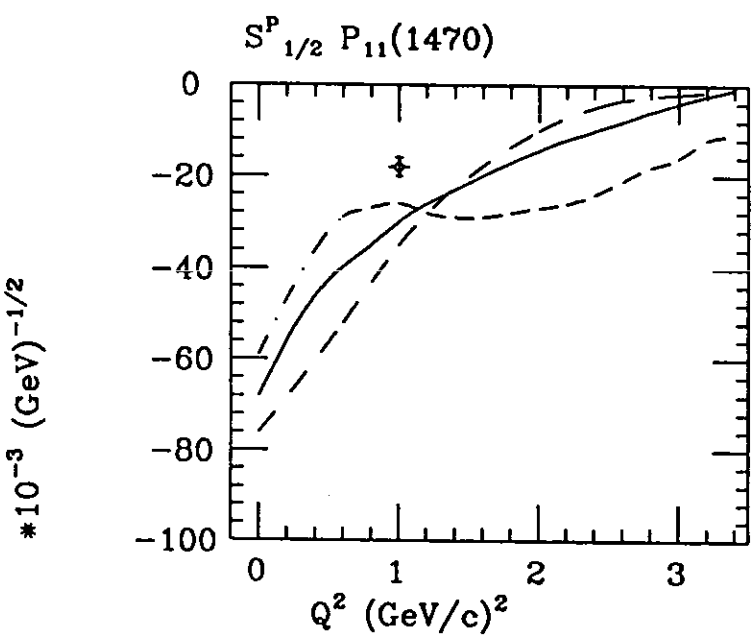
$S^P_{1/2}$ $P_{11}(1470)$
0
−20
−40
−60
−80
−100
0
1
2
3
Q^2 (GeV/c)^2
$*10^{-3}$ (GeV)$^{-1/2}$

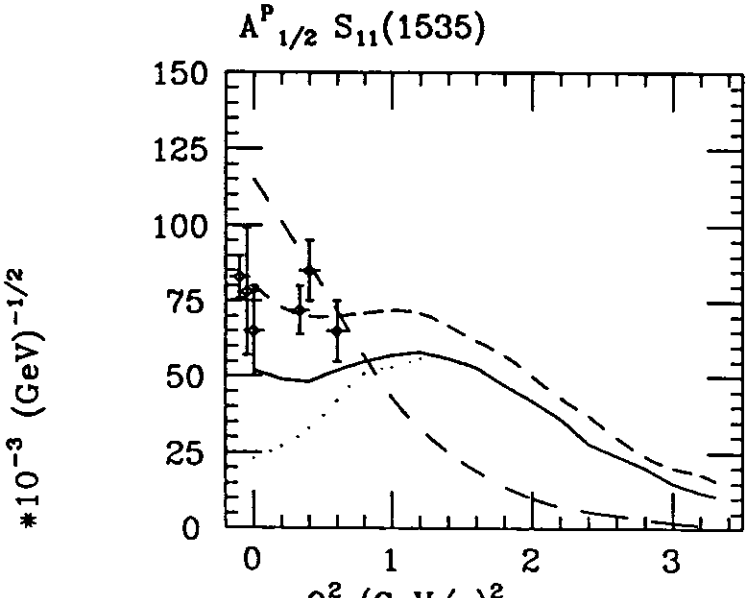
$A^P_{1/2}$ $S_{11}(1535)$
150
125
100
75
50
25
0
0
1
2
3
$*10^{-3}$ (GeV)$^{-1/2}$

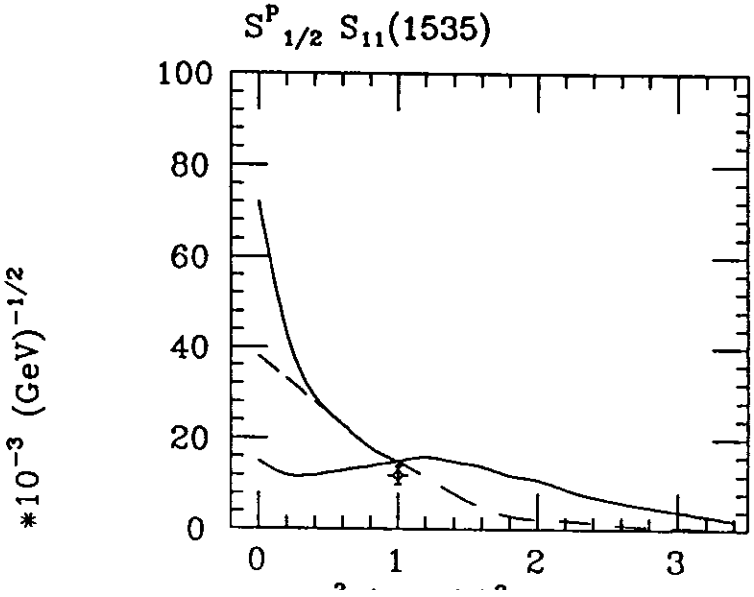
$S^P_{1/2}$ $S_{11}(1535)$
100
80
60
40
20
0
0
1
2
3
$*10^{-3}$ (GeV)$^{-1/2}$

C. Requirements

I. Hardware

I.1. Electron detection and identification

The scattered electron must be detected at angles out to a minimum of 45^0 to satisify the needs of the experiments proposed to study Q^2 up to 3 $(GeV/c)^2$. Detection at larger angles is required for high Q^2 measurements. The electron must be identified in a background of pions. The shower counter and threshold Cerenkov detectors proposed for the forward region of the CLAS will reject more than 99.9% of the pions. For larger angles, the fraction of pions to electrons increases, so that the high Q^2 experiments will also require good pion rejection. For this purpose, it is proposed that one sector of the CLAS be equipped with Cerenkov and shower detectors out to 90^0.

I.2. Hadron detection and identification

Generally the proposed experiments require detection of one charged hadron, either a proton or a π. We expect that the proton and π^+ can be separated by time-of-flight. At the high momentum end of the spectrum, where time-of-flight may begin to fail, the contribution from particles other than protons is expected to be negligible. The detection of π^- produced on neutrons is relatively simple, provided that the electron can be extracted for the event. An additional handle on the pi/e identification is provided by the missing mass reconstruction. Mis-identified particles are unlikely to lead to a sensible missing mass, so that in cases of ambiguity, only one hypothesis is likely to be acceptable.

I.3. Luminosity

The proposals presented here have all calculated rates on the assumption that the CLAS can operate at a luminosity of 10^{34}. Lower luminosities can generally be tolerated, partly at the loss of rate and principally by the reduction of the upper boundary on the Q^2 range of the measurements.

I.4. Beam monitoring

The position of the beam should be monitored and preferably kept stable to a precision consistent with the accuracy of the measurements in the CLAS wire chambers. Stability of beam centroid to 0.1 mm is desirable and seems feasible.

The electron current should be measured to an accuracy of better than 1% to prevent beam current uncertainties from influencing the systematic errors in the experiments. Although the method of monitoring has not been studied, the

desired precision is consistent with results achieved in the past at other electron accelerators.

II. Software Requirements.

The current plan is for a 1000 MIPS processor farm to serve as the fourth level of the CLAS trigger system and eventually to fully process all events. The software in the processor farm must perform numerous tasks. It must identify tracks, determine the momentum, time of flight, mass and charge for each track, reject "bad" events and buffer data for acceptance by an event pool. Data is expected to arrive at the processor farm at a rate of up to a few thousand events per second. Thus the planned processor farm, using an average of a few hundred thousand instructions to filter and reconstruct each event, will meet the needs of the N* collaboration. The initial algorithms developed to perform track recognition and reconstruction require an average of about one hundred thousand instructions per track. Accurate time of flight, mass and charge determination, should require about the same number of instructions. Many events can be rejected before complete track reconstruction begins and will not require much time beyond track identification. However, an estimate of the maximum count rate achievable in each experiment requires a knowledge of the background and reaction characteristics and the event selection criteria.

D. Appendix

Notation Used in Baryon Resonance Proposals

Three-vectors are denoted in boldface, and four-vectors in plain font,eg. P = (E,**P**)

* : denotes all the quantities below in center-of-mass

$\rightarrow$: indicates polarized particle (eg.$\vec{p}_e$)

E : incident electron energy.

E′ : scattered electron energy.

(ν,q) : energy transfer (E - E′), and three momentum transfer.

q^2 : four momentum transfer.

Q^2 : $-q^2$

W : total system invariant mass. $W^2 = S = (q + p_I)^2$

K_L : equivalent photon energy. $K_L = (W^2 - M^2)/2M$

ϵ : virtual photon polarization parameter.

$$\epsilon = (1 - 2\frac{\nu^2 - q^2}{q^2} tan^2 \frac{\theta_m}{2})^{-1}$$

$\Gamma(E, \Omega_e)$: virtual photon flux in interval $dEd\Omega_e$

$$\Gamma(E, \Omega_e) = \frac{\alpha K_L}{2\pi^2 Q^2} \frac{E'}{E} \frac{1}{1 - \epsilon}$$

$\Gamma(Q^2, \nu)$: virtual photon flux in interval $dQ^2 d\nu_e$

$$\Gamma(Q^2, \nu) = \frac{\pi W}{EE'M} \Gamma(E, \Omega_e)$$

For an unpolarized beam and target, the electroproduction of a single meson can be written

$$\frac{d\sigma}{d\Omega_e dE_e d\Omega_m} = \Gamma_v[\frac{d\sigma_T}{d\Omega_m} + \epsilon\frac{d\sigma_L}{d\Omega_m} + \epsilon cos2\phi_m^* \frac{d\sigma_{TT}}{d\Omega_m} + \sqrt{\epsilon(\epsilon+1)}cos\phi_m^* \frac{d\sigma_{LT}}{d\Omega_m}]$$

The electroproduction cross section can be characterized in terms of six complex helicity amplitudes H_i, where $H_{1\to4}$ are due to transverse and $H_{5,6}$ are due to longitudinal photons. For example, the transverse and longitudinal virtual photon cross sections can be written

$$\frac{d\sigma_T}{d\Omega_m} = \frac{q}{2k}\sum_{n=1}^{4}|H_i|^2 \qquad \frac{d\sigma_L}{d\Omega_m} = \frac{q}{k}\sum_{n=5}^{6}|H_i|^2$$

The amplitudes H_i can be expanded in terms of Legendre polynomials:

$$H_1 = \frac{1}{2}\sqrt{2}sin(\theta_m)cos(\theta_m/2)\sum_{l=4}^{\infty}(B_{l+} - B_{(l+1)-})(P_l'' - P_{l+1}'')$$

$$H_2 = \sqrt{2}cos(\theta_m/2)\sum_{l=4}^{\infty}(A_{l+} - A_{(l+1)-})(P_l' - P_{l+1}')$$

$$H_3 = \frac{1}{2}\sqrt{2}sin(\theta_m)sin(\theta_m/2)\sum_{l=4}^{\infty}(B_{l+} + B_{(l+1)-})(P_l'' + P_{l+1}'')$$

$$H_4 = \sqrt{2}sin(\theta_m)\sum_{l=4}^{\infty}(A_{l+} + A_{(l+1)-})(P_l' + P_{l+1}')$$

$$H_5 = \sqrt{2}cos(\theta_m/2)\sum_{l=4}^{\infty}(C_{l+} - C_{(l+1)-})(P_l' - P_{l+1}')$$

$$H_6 = \sqrt{2}sin(\theta_m/2)\sum_{l=4}^{\infty}(C_{l+} + C_{(l+1)-})(P_l' + P_{l+1}')$$

where the coefficients $A_{l\pm}$, $B_{l\pm}$, and $C_{l\pm}$ are helicity elements. The helicity elements are related to the CGLN amplitudes as follows:

$$M_{l+} = [2(l+1)]^{-1}(2A_{l+} - (l+2)B_{l+})$$

$$E_{l+} = [2(l+1)]^{-1}(2A_{l+} + lB_{l+})$$

$$M_{l+1,-} = [2(l+1)]^{-1}(2A_{l+1,-} + lB_{l+1,-})$$

$$E_{l+1,-} = [2(l+1)]^{-1}(-2A_{l+1,-} + (l+2)B_{l+1,-})$$

$$S_{l+} = [l+1]^{-1}(p^*{}_m/Q^2)(C_{l+})$$

$$S_{l+1,-} = [l+1]^{-1}(p^*{}_m/Q^2)(C_{l+1,-})$$

The strong interaction part of the helicity elements can be separated out yielding the electromagnetic helicity amplitudes $A_{1/2}$ and $A_{3/2}$ according to the following relationship:

$$A_{l\pm} = \mp K C^I_{\pi N} A_{1/2}$$

$$B_{l\pm} = \pm K \sqrt{\frac{16}{(2j-1)(2j+3)}} C^I_{\pi N} A_{3/2}$$

$$K = \sqrt{\frac{1}{(2j+1)\pi} \frac{k}{q} \frac{M}{W_R} \frac{\Gamma_\pi}{\Gamma} \frac{1}{\Gamma}}$$

where $C^I_{\pi N}$ are isospin coefficients. For a resonant state

$$\sigma^T = (C^I_{\pi N})^2 \frac{M}{W_R} \frac{\Gamma_\pi}{\Gamma^2} (|A_{1/2}|^2 + |A_{3/2}|^2)$$

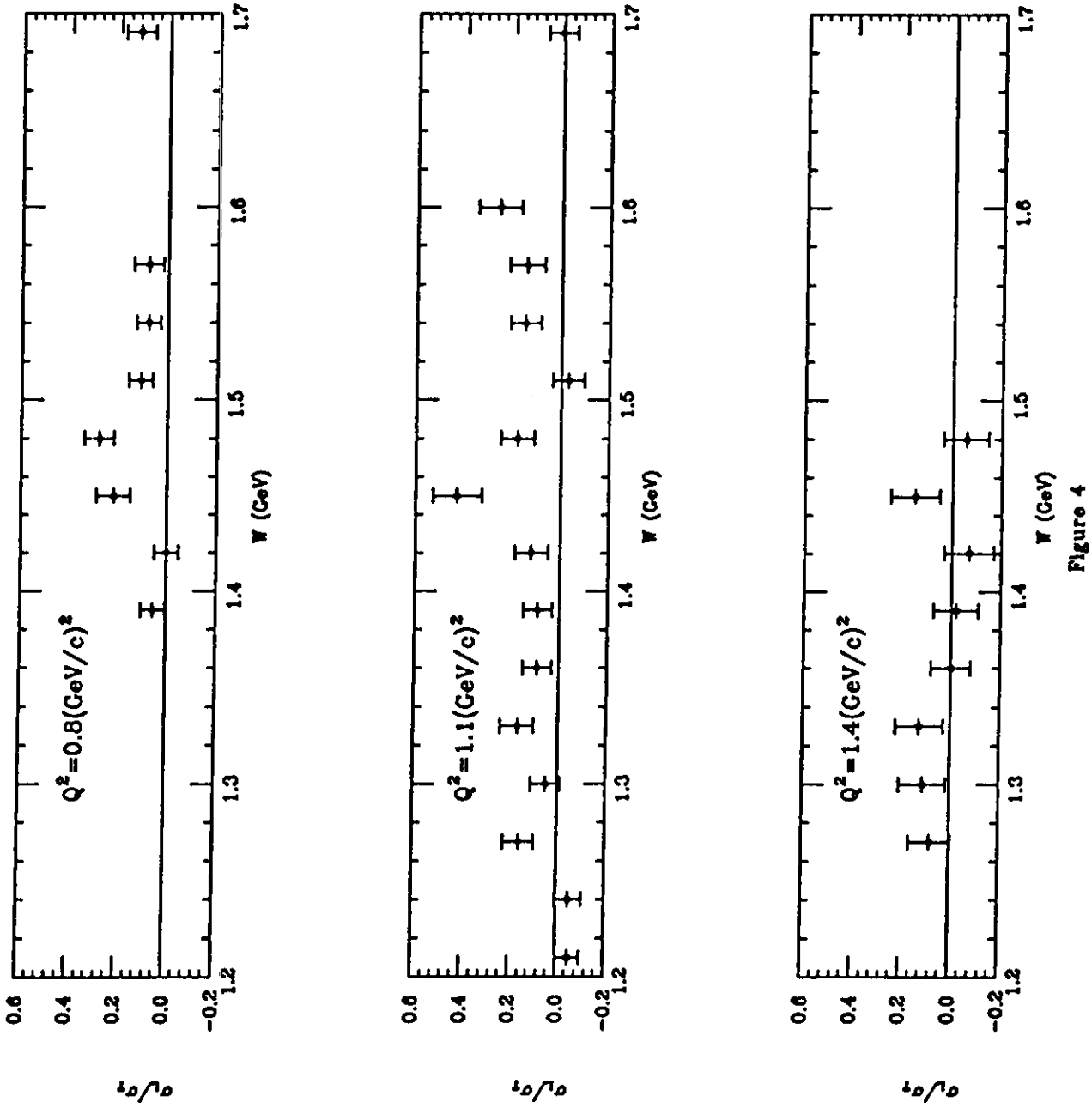
Q^2=0.8(GeV/c)^2
Q^2=1.1(GeV/c)^2
Q^2=1.4(GeV/c)^2
W (GeV)
σ_L/σ_T
0.6
0.4
0.2
0.0
-0.2
1.2
1.3
1.4
1.5
1.6
1.7

Figure 4

Electroproduction: π^+ at Q^2 = 1.0 (GeV/c)^2, W = 1.49 – 1.52 GeV

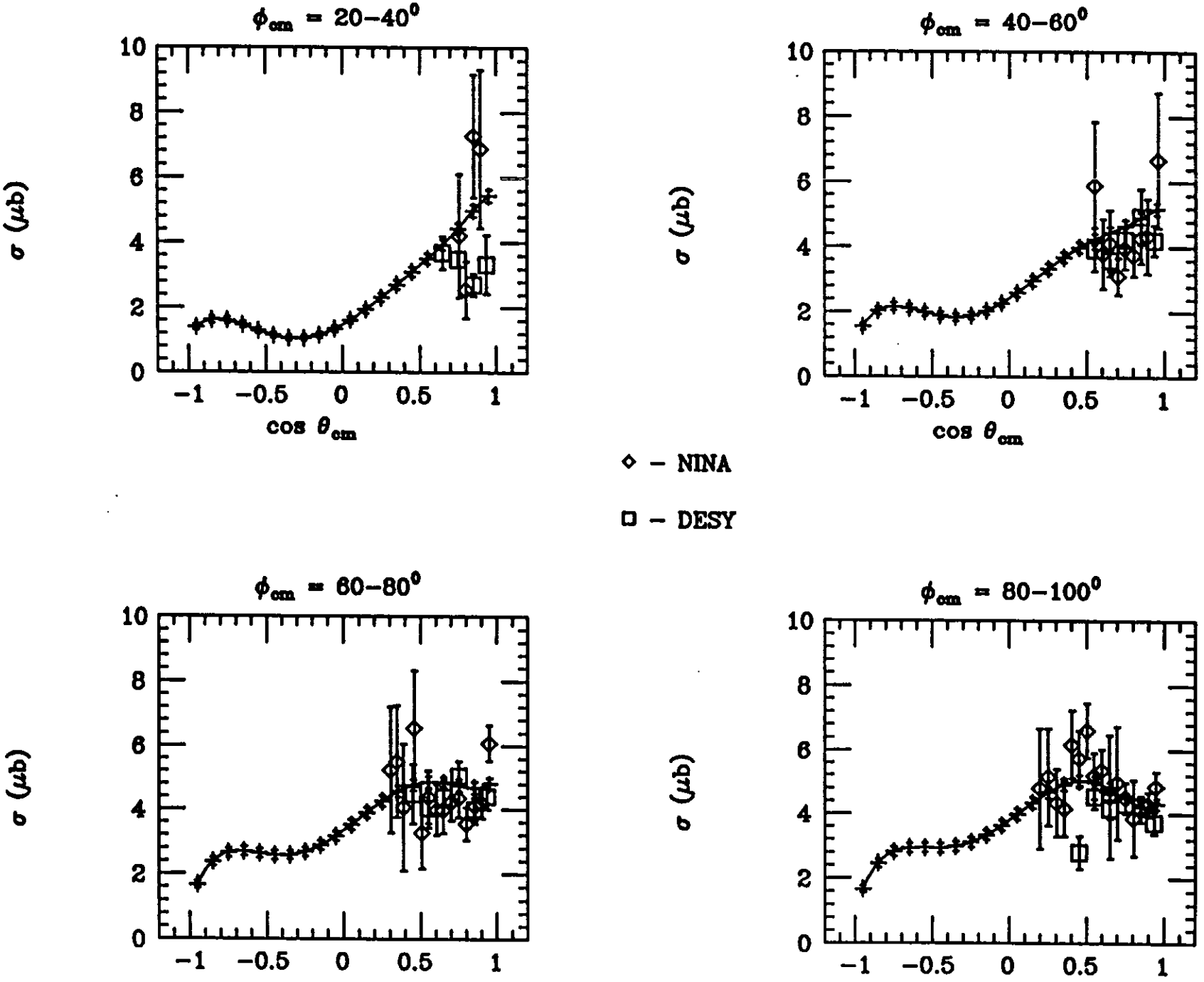

Electroproduction: π^+ at Q^2 = 1.0 (GeV/c)^2, W = 1.49 – 1.52 GeV

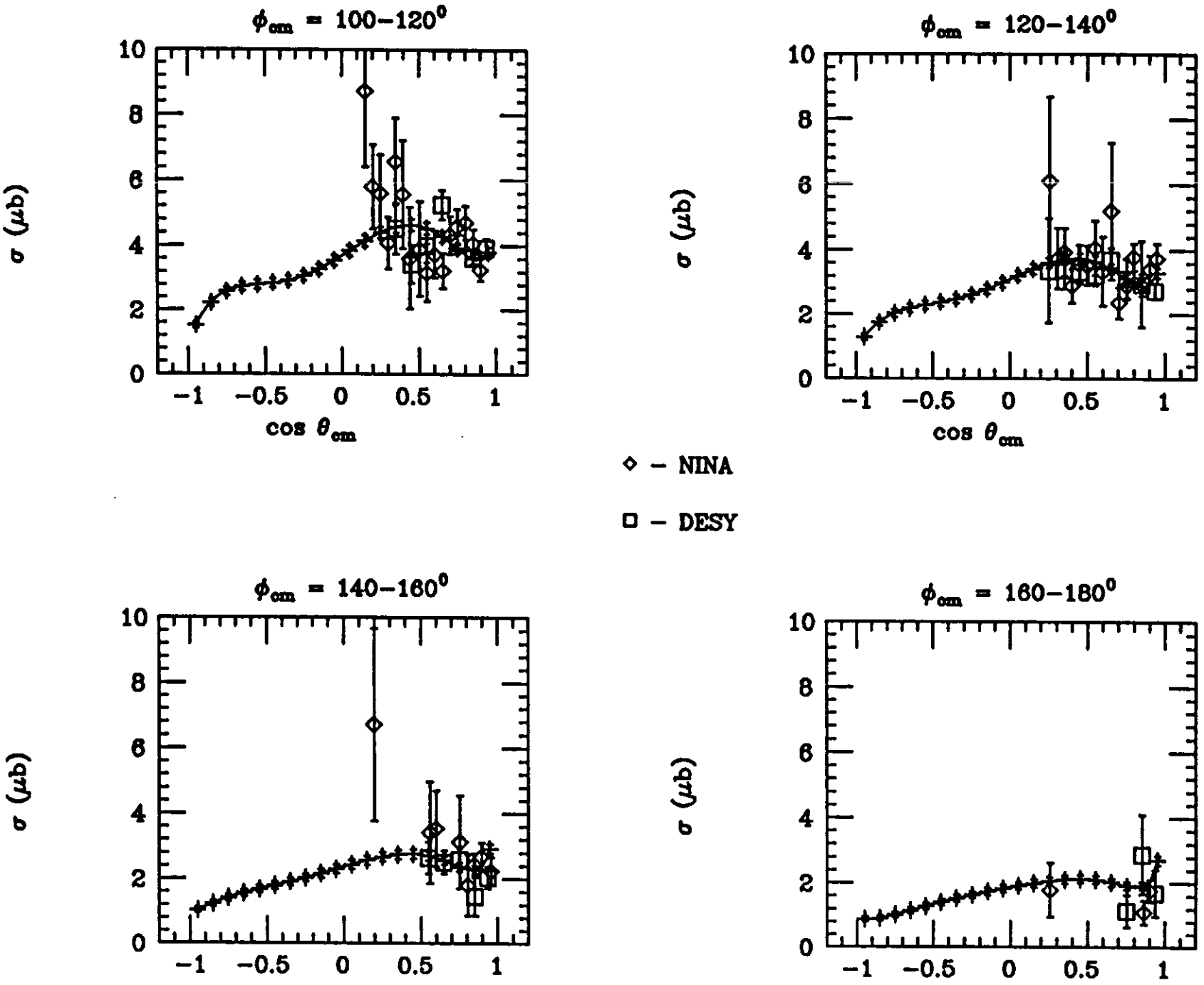

$p(e,e\,\pi^+)n$, $E_0 = 4.0$ GeV, $Q^2 = 2$ (GeV/c)^2

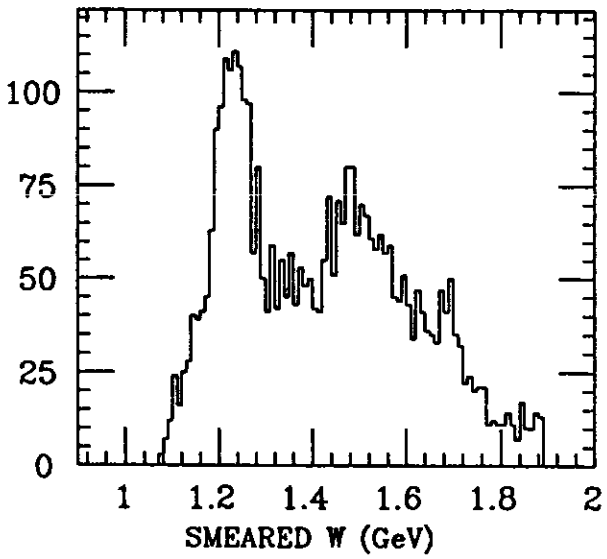

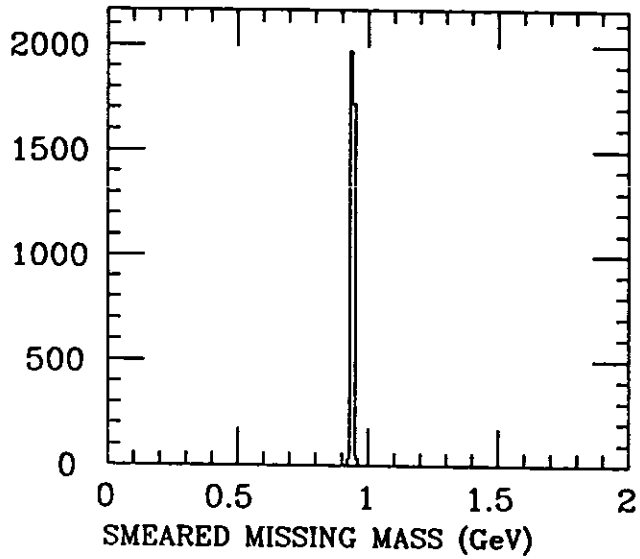

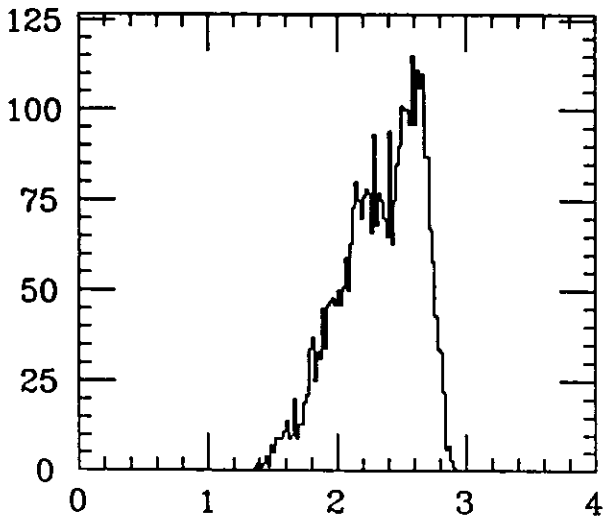

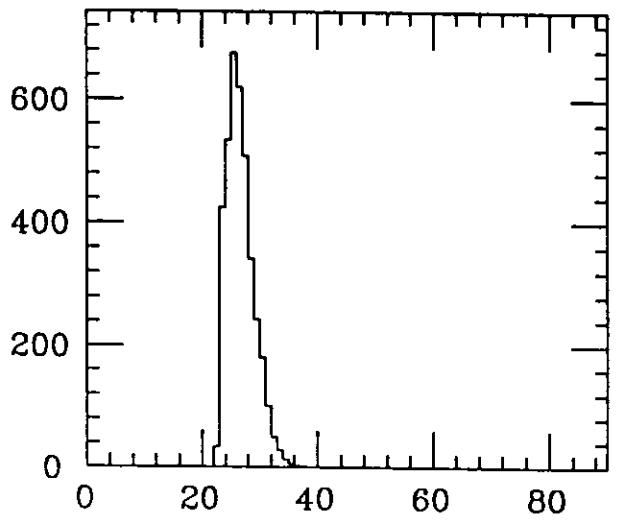

$p(e,e\,\pi^+)n$, $E_0 = 4.0$ GeV, $Q^2 = 2$ $(GeV/c)^2$

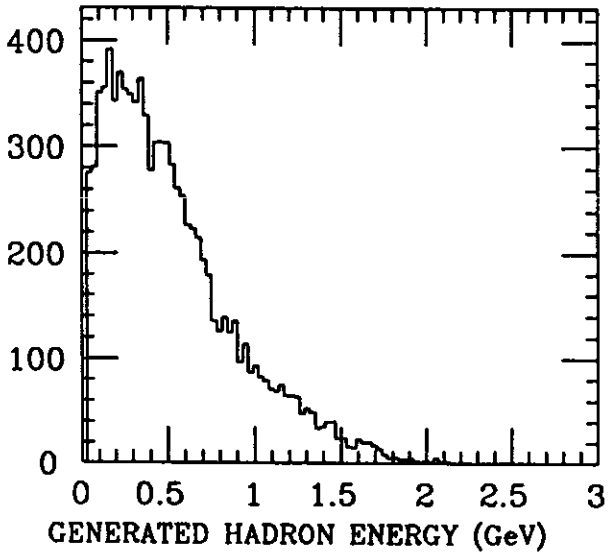

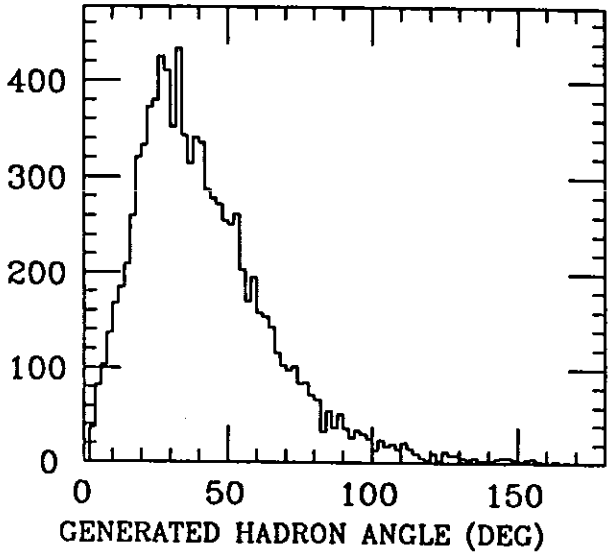

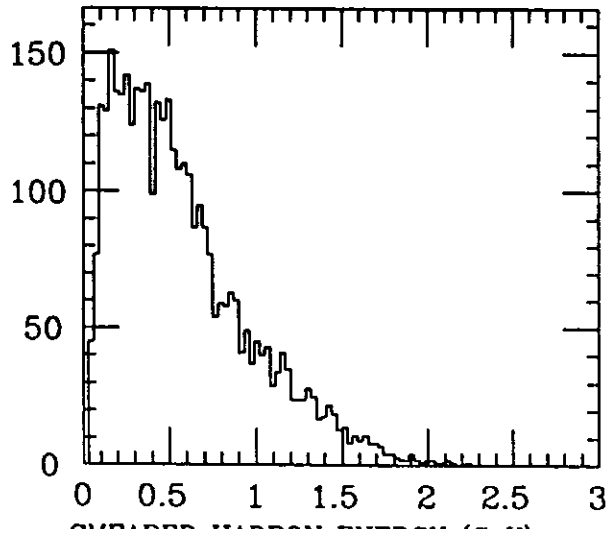

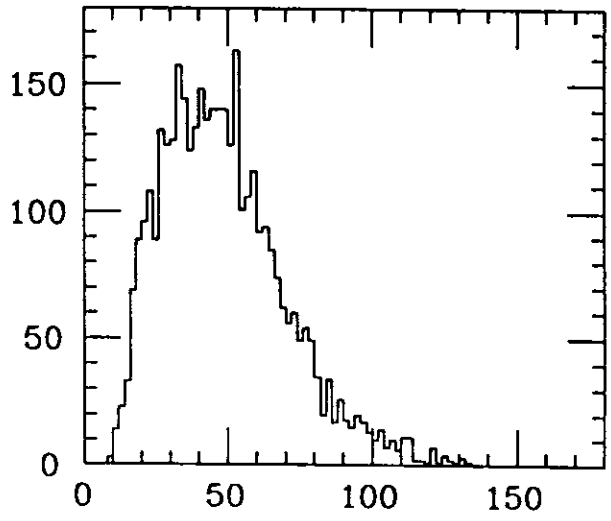

$p(e,e\,\pi^+)n$, $E_0 = 4.0$ GeV, $Q^2 = 2$ $(GeV/c)^2$

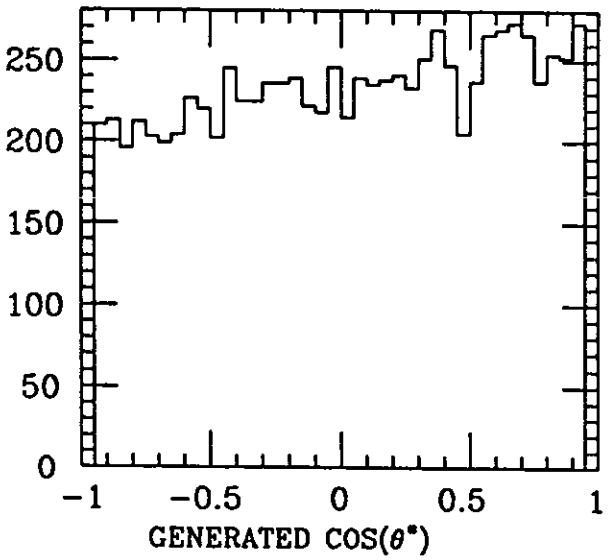

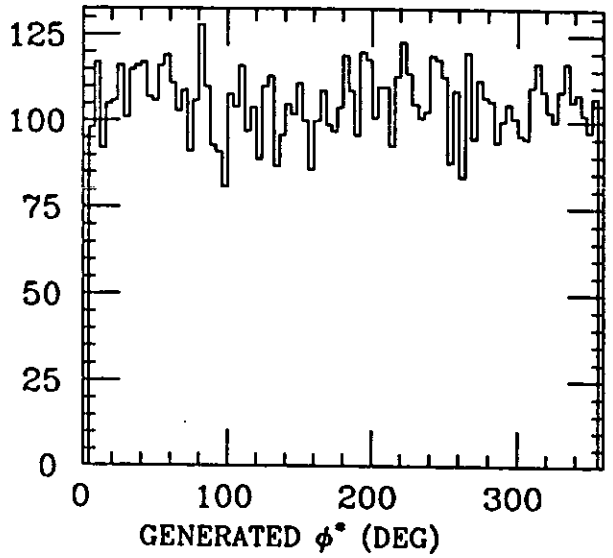

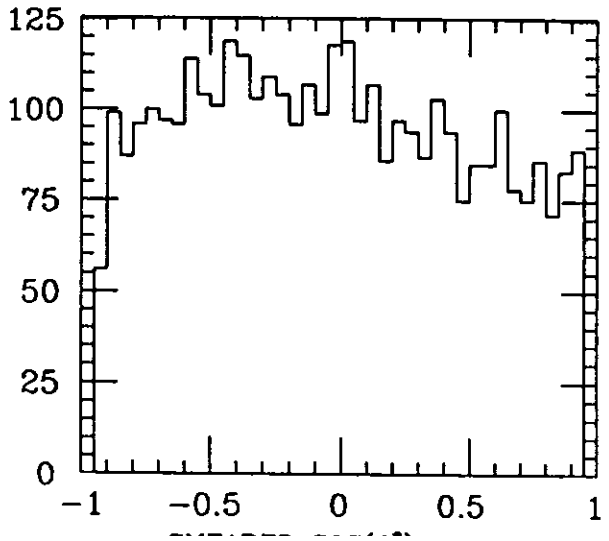

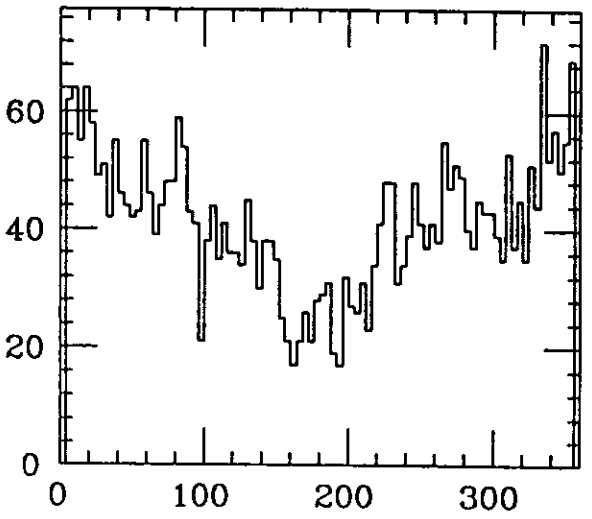

$p(e,e\ p)\pi^0$, $E_0 = 4.0$ GeV, $Q^2 = 2$ $(GeV/c)^2$

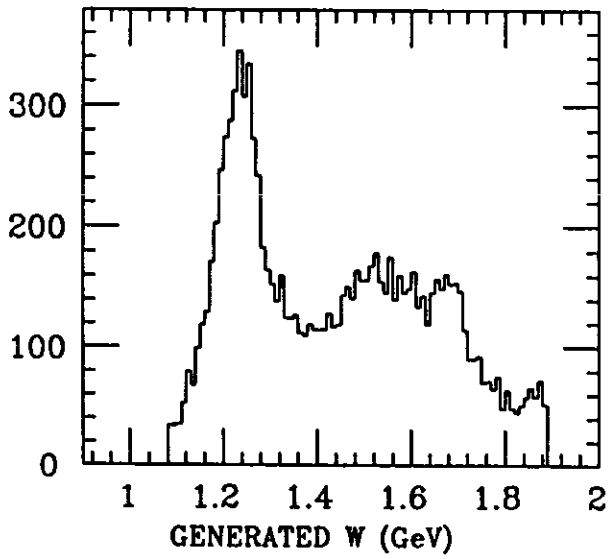

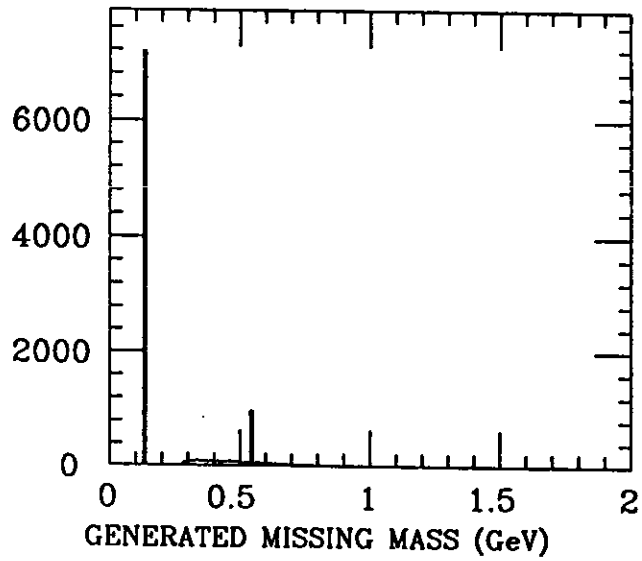

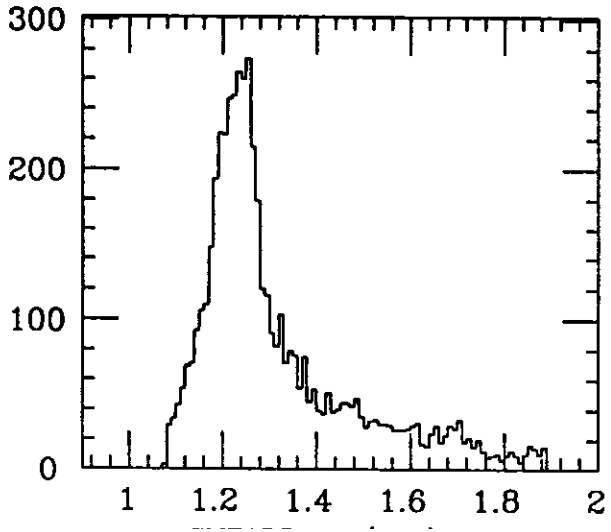

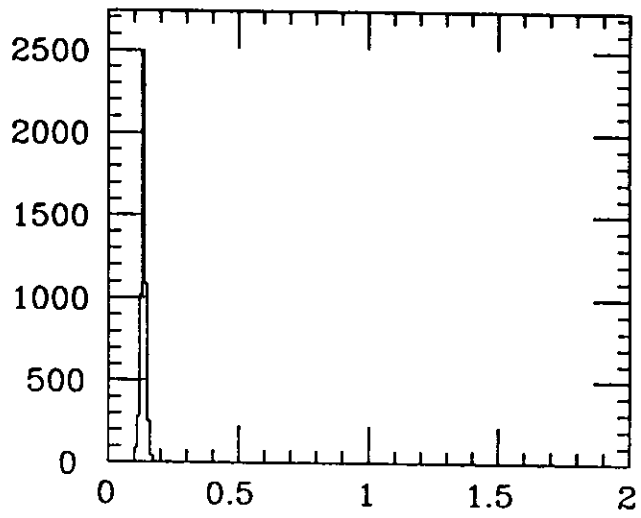

$p(e,e\ p)\pi^0$, $E_0 = 4.0$ GeV, $Q^2 = 2$ (GeV/c)^2

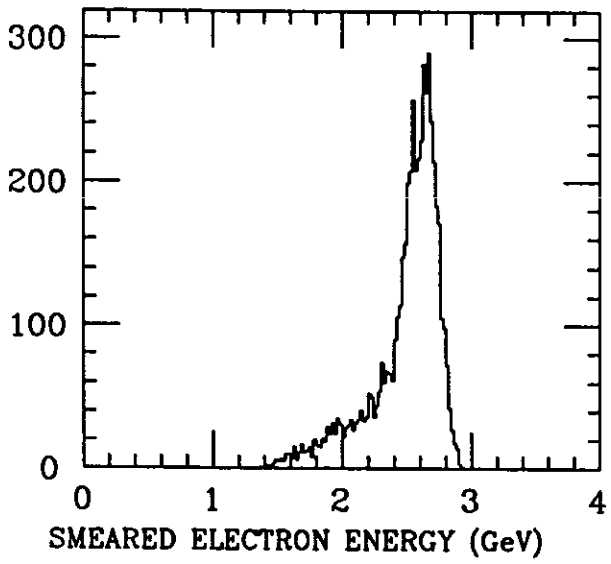

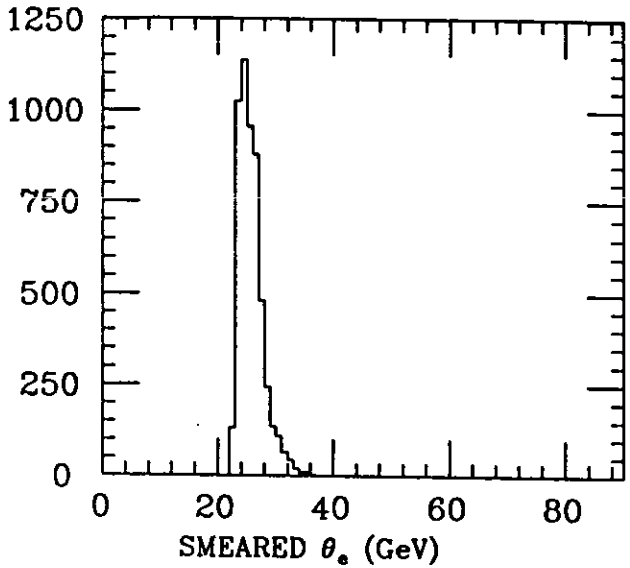

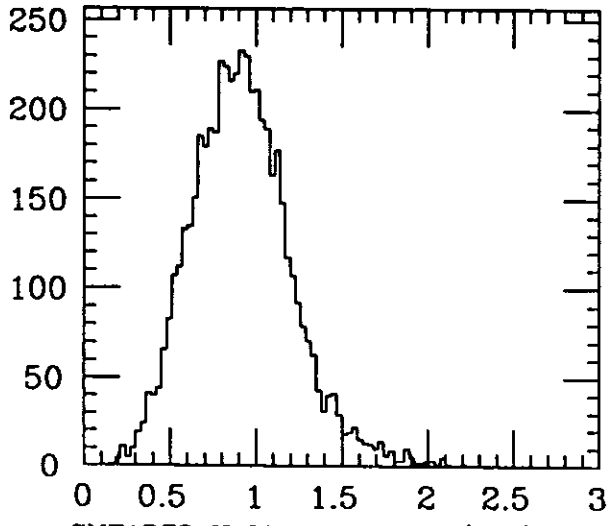

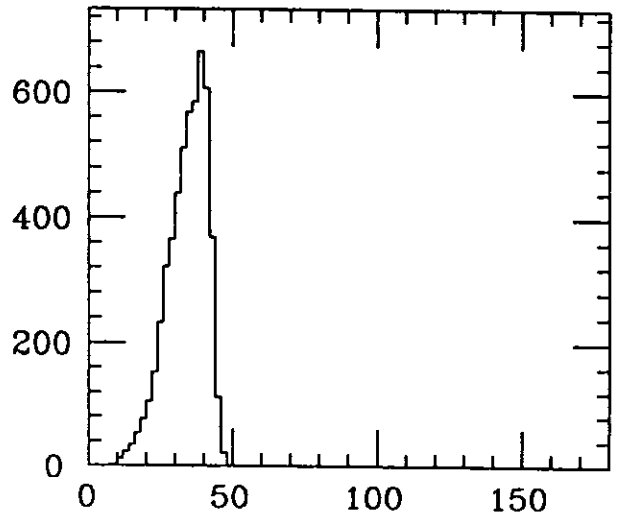

$p(e,e\ p)\pi^0$, $E_0 = 4.0$ GeV, $Q^2 = 2$ $(GeV/c)^2$

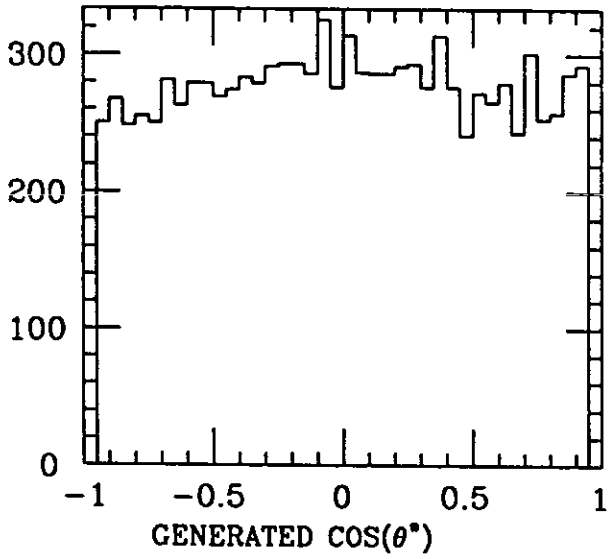

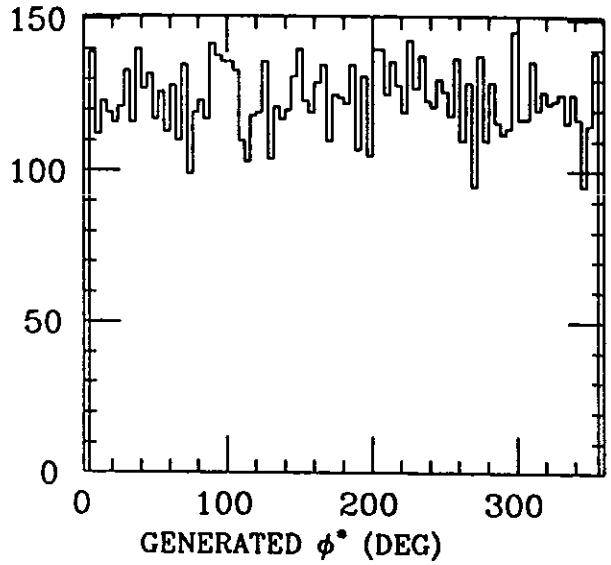

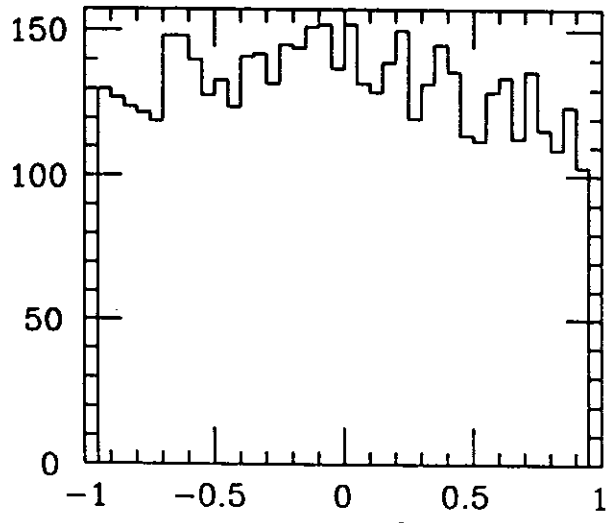

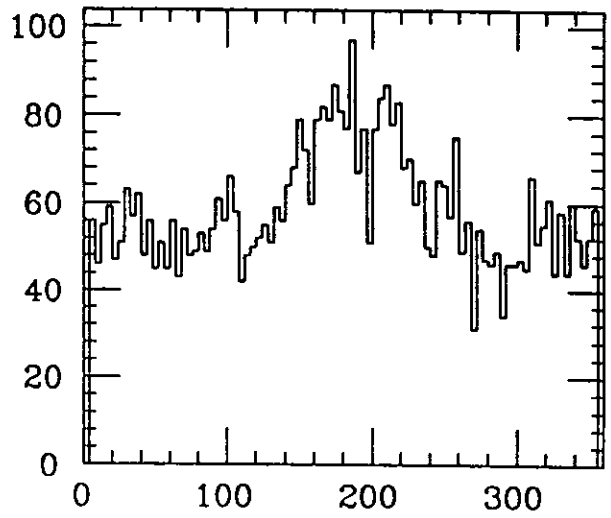

$p(e, e' \pi^+)n$, $E_0 = 4$ GeV, S11(1530)

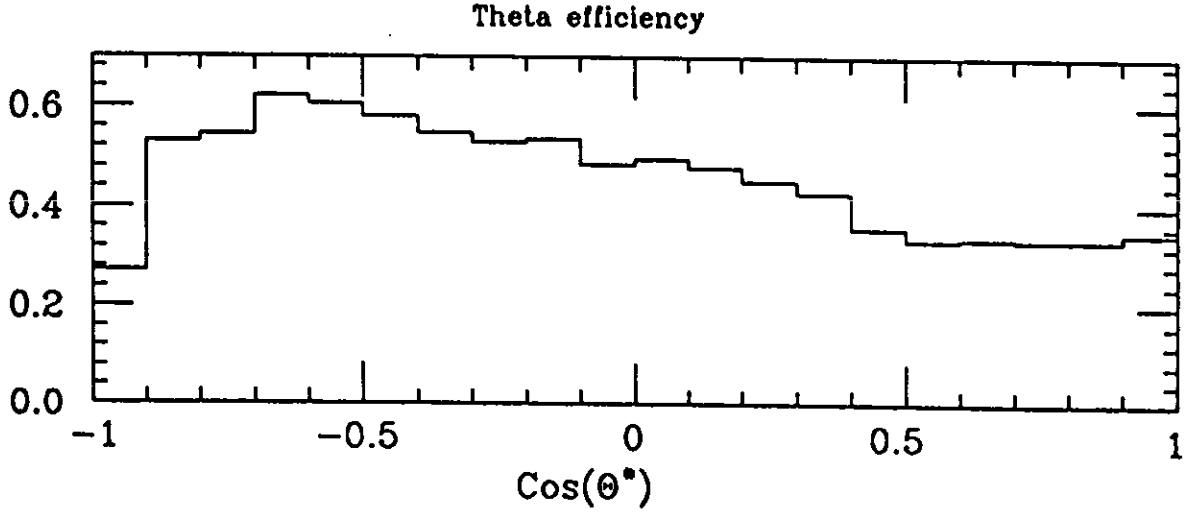

30000 Events, 7-OCT-1989
Negatives bend toward axis
Missing mass limits: 0.90 0.98

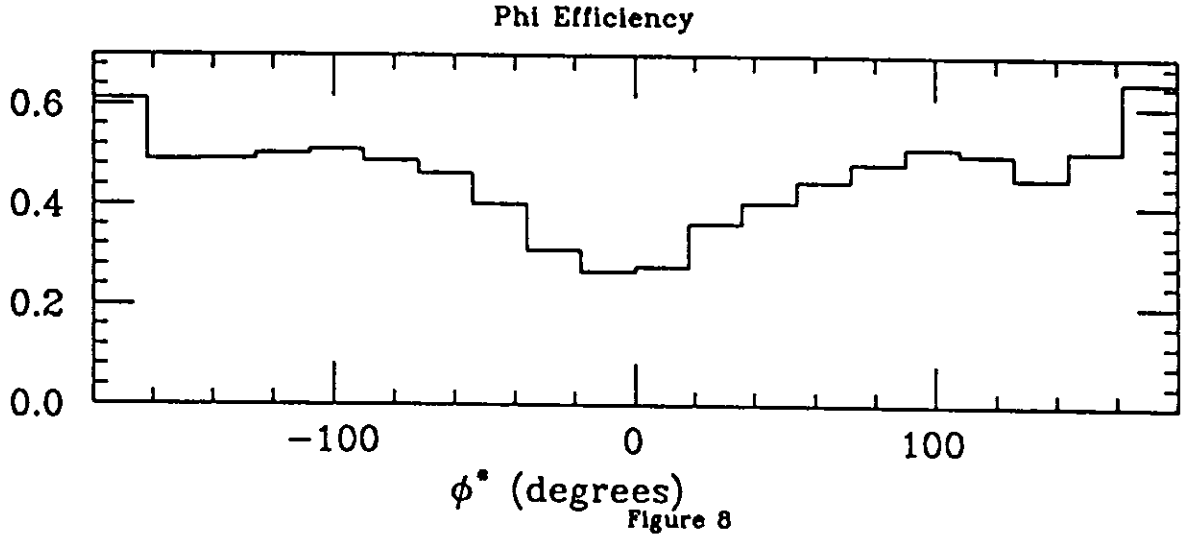

Figure 8

$d(e,e\,\pi^+)nn \quad E_0 = 4.0\ \text{GeV} \quad Q^2 = 2\ (\text{GeV/c})^2$

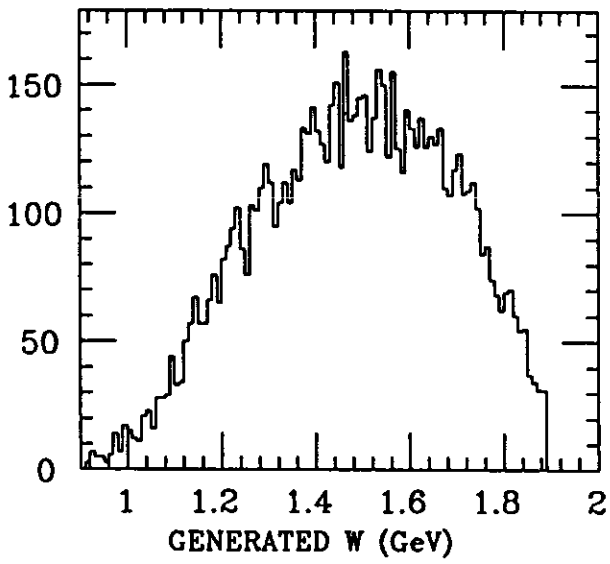

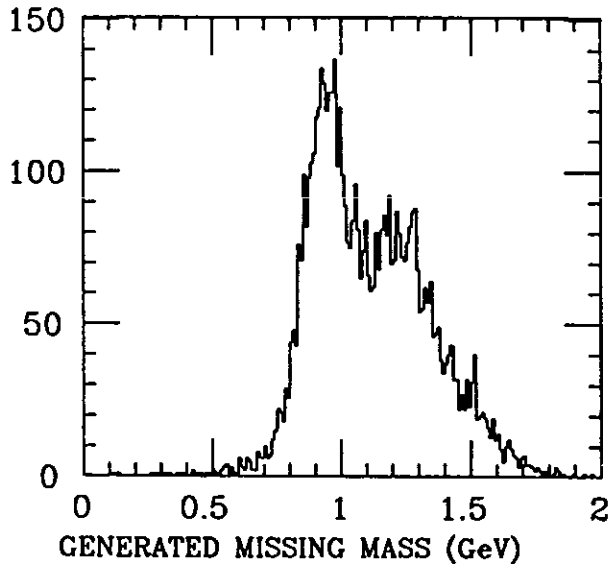

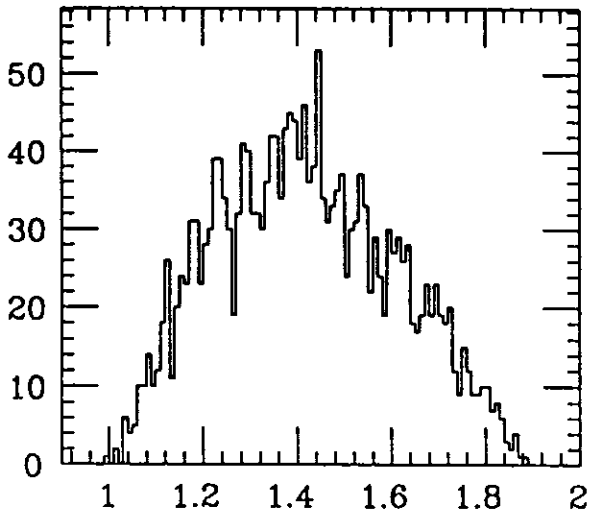

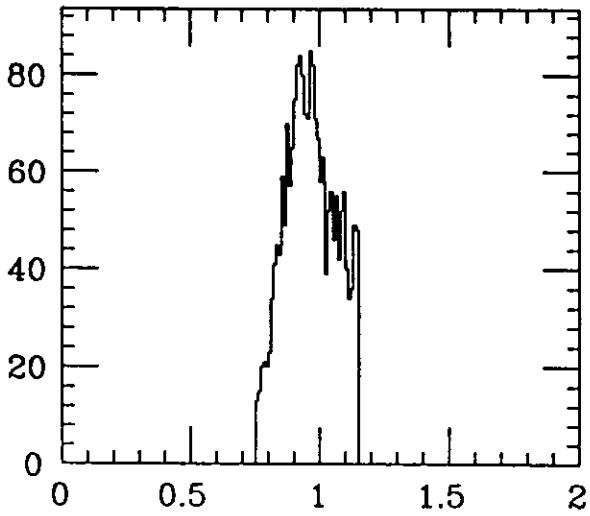

$d(e,e\,\pi^+)nn \quad E_0 = 4.0\ \text{GeV} \quad Q^2 = 2\ (\text{GeV/c})^2$

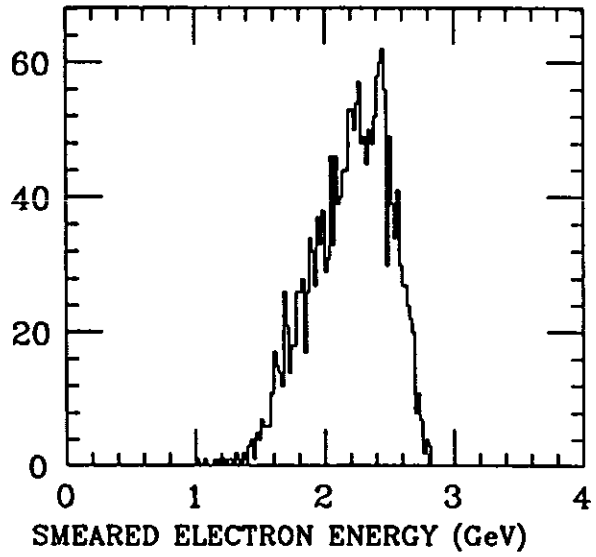

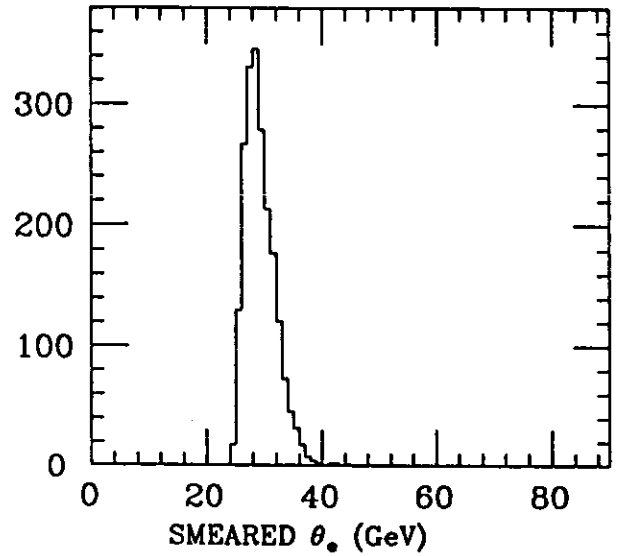

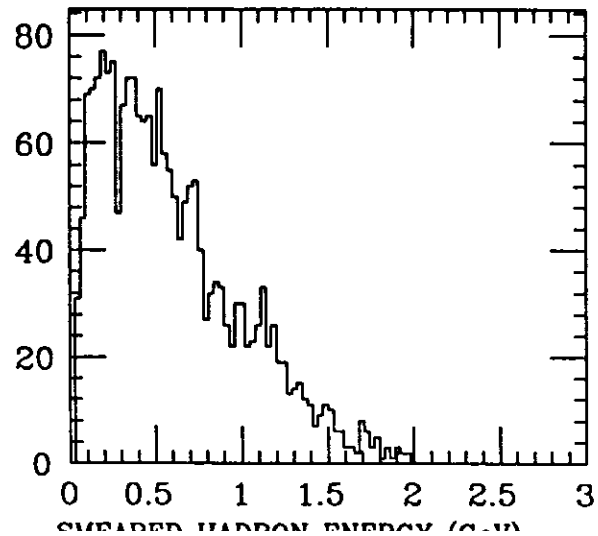

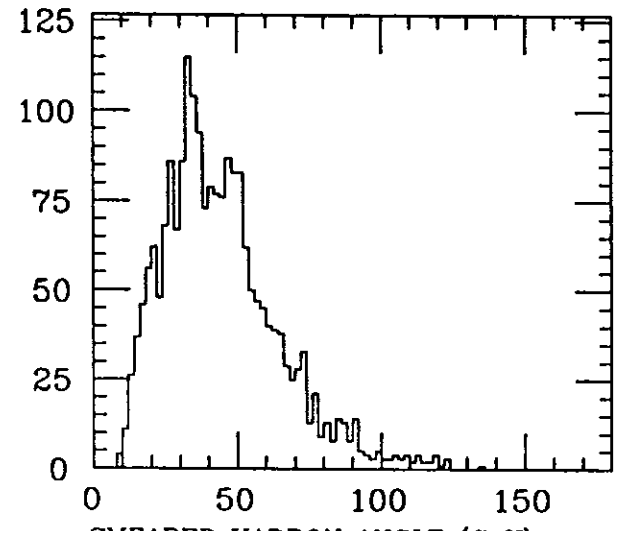

$d(e,e\,\pi^+)nn \quad E_0 = 4.0\ \text{GeV} \quad Q^2 = 2\ (\text{GeV/c})^2$

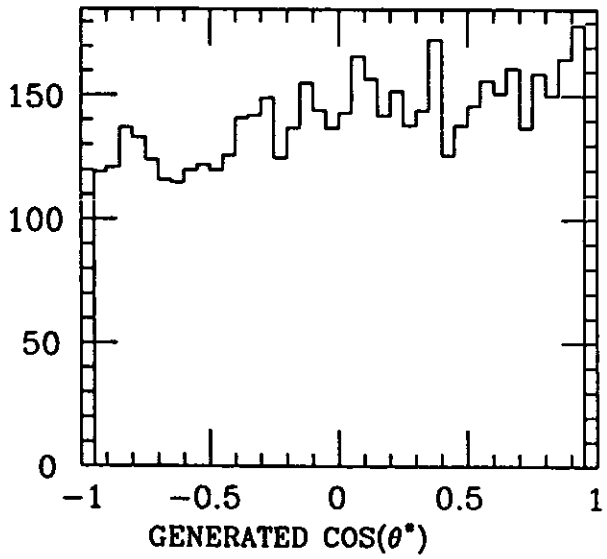

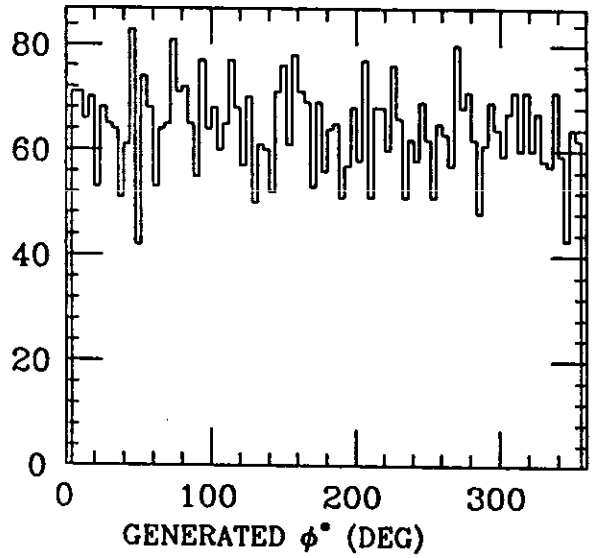

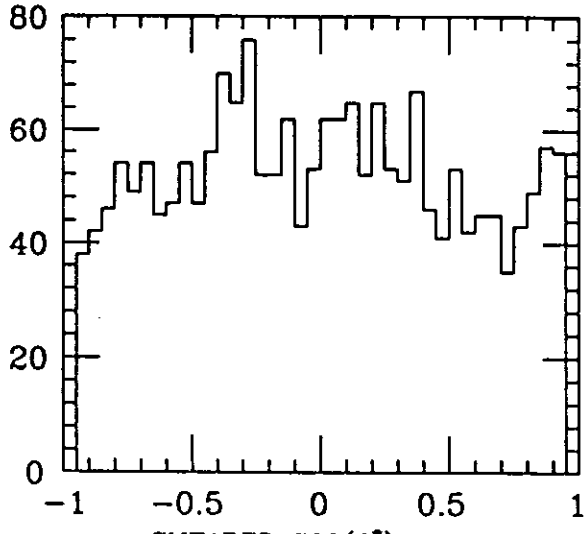

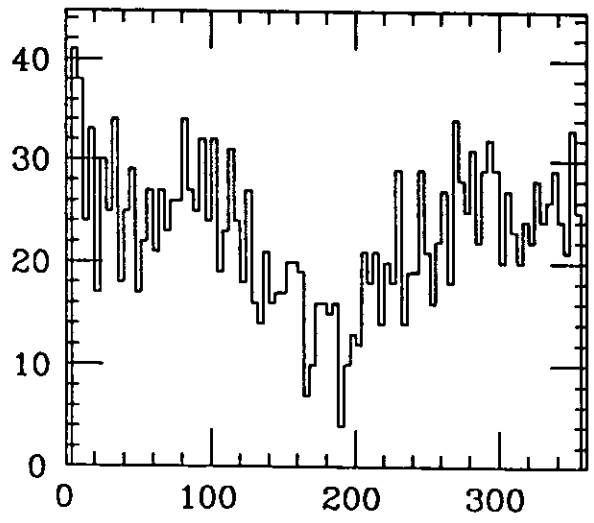

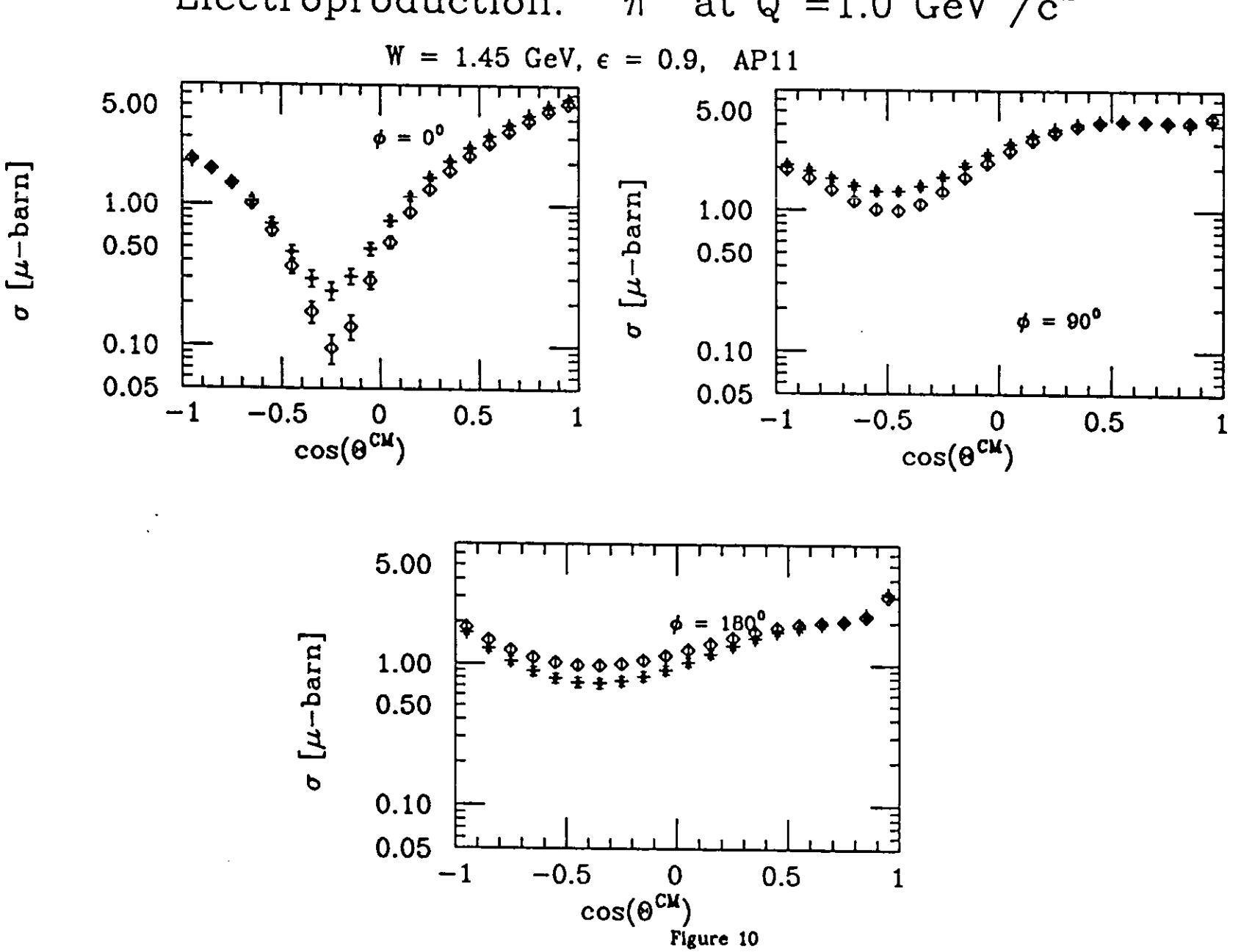
Electroproduction: π^+ at Q^2=1.0 GeV^2/c^2
W = 1.45 GeV, ε = 0.9, AP11
σ [μ-barn]
5.00
1.00
0.50
0.10
0.05
φ = 0°
φ = 90°
φ = 180°
−1
−0.5
0
0.5
1
cos(θ^{CM})

Figure 10

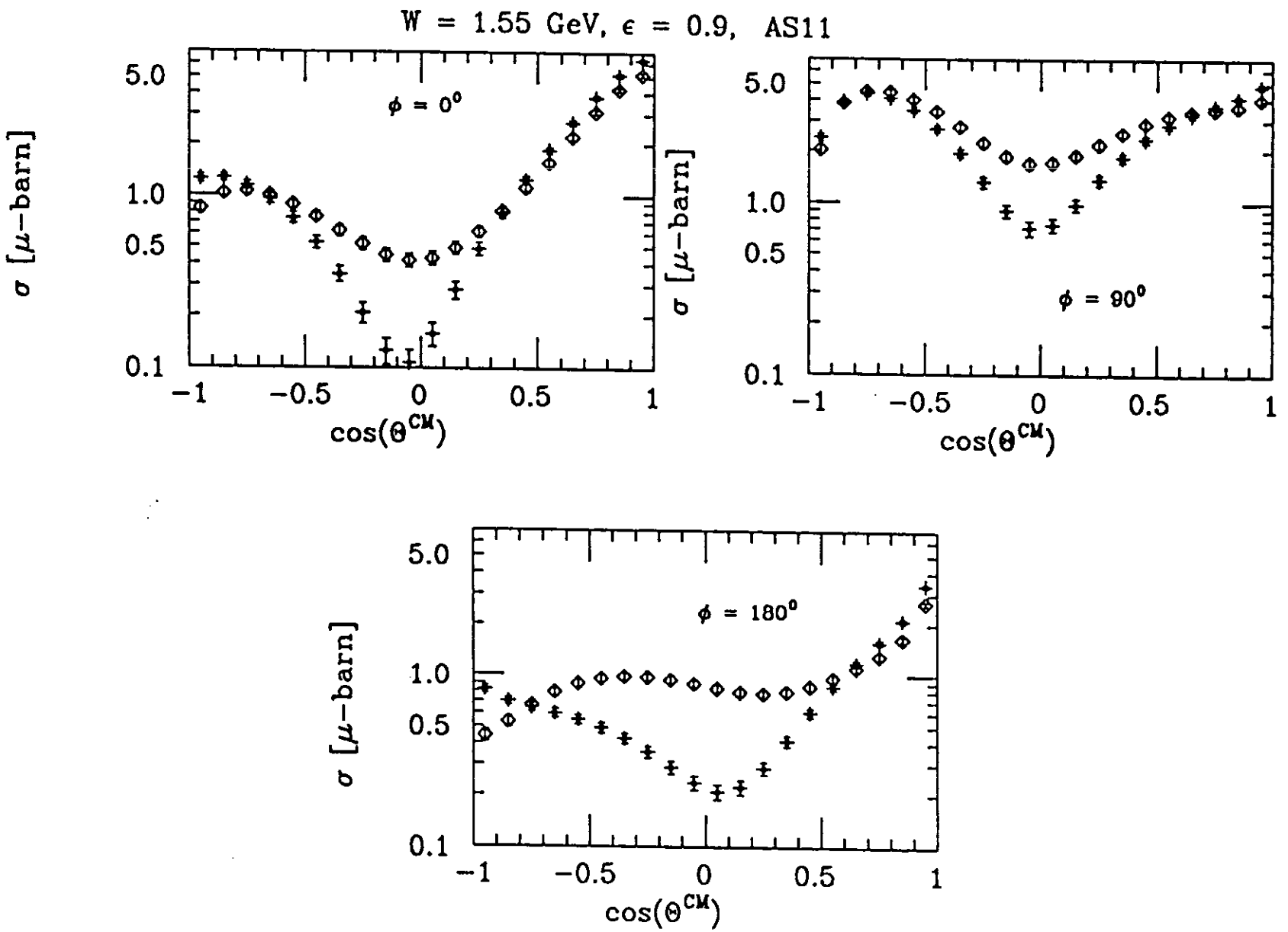
Electroproduction: π^+ at Q^2=1.0 GeV^2/c^2
W = 1.55 GeV, ε = 0.9, AS11
σ [μ-barn]
5.0
1.0
0.5
0.1
φ = 0°
φ = 90°
φ = 180°
−1
−0.5
0
0.5
1
cos(θ^{CM})

Figure 11

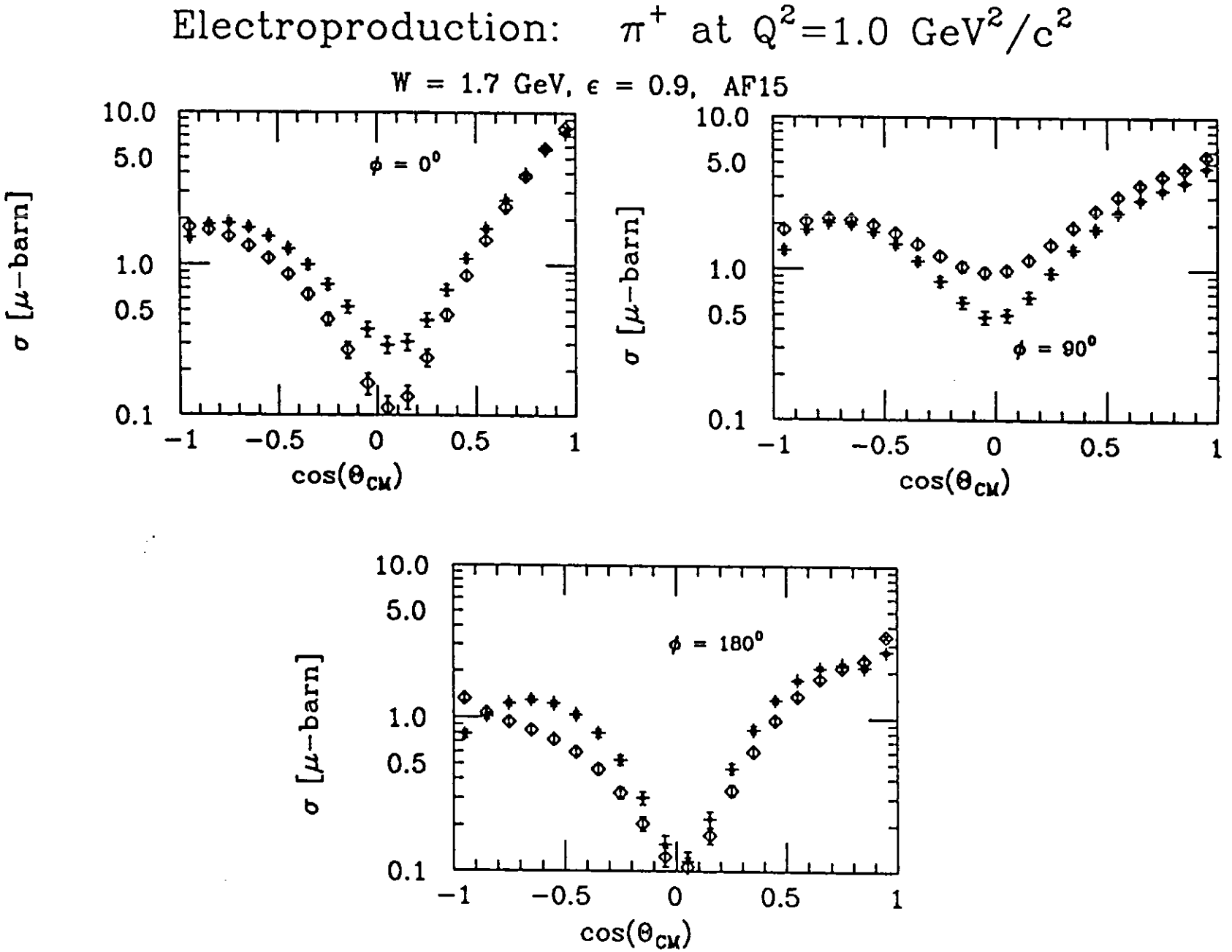
Electroproduction: π^+ at Q^2=1.0 GeV^2/c^2
W = 1.7 GeV, ε = 0.9, AF15
σ [μ-barn]
10.0
5.0
1.0
0.5
0.1
φ = 0°
φ = 90°
φ = 180°
−1
−0.5
0
0.5
1
cos(θCM)

Figure 12